



# Strong Stability Preserving IMEX Methods for Partitioned Systems of Differential Equations

Giuseppe Izzo<sup>1</sup> · Zdzisław Jackiewicz<sup>2,3</sup>

Received: 9 May 2021 / Revised: 11 July 2021 / Accepted: 13 July 2021 /  
Published online: 30 October 2021  
© The Author(s) 2021

## Abstract

We investigate strong stability preserving (SSP) implicit-explicit (IMEX) methods for partitioned systems of differential equations with stiff and nonstiff subsystems. Conditions for order  $p$  and stage order  $q = p$  are derived, and characterization of SSP IMEX methods is provided following the recent work by Spijker. Stability properties of these methods with respect to the decoupled linear system with a complex parameter, and a coupled linear system with real parameters are also investigated. Examples of methods up to the order  $p = 4$  and stage order  $q = p$  are provided. Numerical examples on six partitioned test systems confirm that the derived methods achieve the expected order of convergence for large range of stepsizes of integration, and they are also suitable for preserving the accuracy in the stiff limit or preserving the positivity of the numerical solution for large stepsizes.

**Keywords** Partitioned systems of differential equations · SSP property · IMEX general linear methods · Construction of highly stable methods

**Mathematics Subject Classification** 65L05

## 1 Introduction

Strong stability preserving (SSP) implicit-explicit (IMEX) Runge-Kutta methods for differential problems in additive form have been investigated in recent literature [9, 26].

In this manuscript, we consider a partitioned system of ordinary differential equations (ODEs)

---

✉ Giuseppe Izzo  
giuseppe.izzo@unina.it  
Zdzisław Jackiewicz  
jackiewicz@asu.edu

<sup>1</sup> Member of the INdAM Research group GNCS, Dipartimento di Matematica e Applicazioni “R.Caccioppoli”, Università degli Studi di Napoli Federico II, 80126 Napoli, Italy

<sup>2</sup> School of Mathematical and Statistical Sciences, Arizona State University, Tempe, AZ 85287, USA

<sup>3</sup> Faculty of Applied Mathematics, AGH University of Science and Technology, Kraków, Poland

$$\begin{cases} x'(t) = f(x(t), z(t)), & x(t_0) = x_0, \\ z'(t) = g(x(t), z(t)), & z(t_0) = z_0, \end{cases} \quad (1)$$

$t \in [t_0, t_{\text{end}}]$ , where the solution vector is separated into two components  $x$  and  $z$ . We assume that the first subsystem of (1) corresponding to the function  $f : \mathbb{R}^m \times \mathbb{R}^n \rightarrow \mathbb{R}^m$  is non-stiff, and the second subsystem of (1) corresponding to the function  $g : \mathbb{R}^m \times \mathbb{R}^n \rightarrow \mathbb{R}^n$  is stiff. Introducing the notation

$$y(t) = \begin{bmatrix} x(t) \\ z(t) \end{bmatrix}, \quad F(y(t)) = \begin{bmatrix} f(x(t), z(t)) \\ g(x(t), z(t)) \end{bmatrix} = \begin{bmatrix} f(y(t)) \\ g(y(t)) \end{bmatrix}, \quad y_0 = \begin{bmatrix} x_0 \\ y_0 \end{bmatrix},$$

the system (1) can be written in a more compact form

$$y'(t) = F(y(t)), \quad y(t_0) = y_0, \quad (2)$$

$t \in [t_0, t_{\text{end}}]$ , corresponding to the function  $F : \mathbb{R}^{m+n} \rightarrow \mathbb{R}^{m+n}$ .

The problem (1) will be integrated by the class of IMEX methods, where the first subsystem of (1) is integrated by explicit general linear method (GLM), and the second subsystem of (1) is integrated by diagonally implicit GLM. These methods for subsystems of (1) and the overall IMEX scheme, are defined in Sect. 2. In Sect. 3, we discuss stage order and order conditions for IMEX methods, and prove that the IMEX scheme has order  $p$  and stage order  $q = p$  if and only if the explicit and implicit “components” of the scheme have order  $p$  and stage order  $q = p$ . Stability properties of IMEX GLMs are investigated in Sect. 4. In Sect. 5, we define the SSP property of IMEX methods. A large class of transformed IMEX GLMs is defined in Sect. 6. In Sect. 7, we discuss the characterization of SSP IMEX methods, which is based on the recent work by Spijker [44]. Construction of transformed SSP IMEX GLMs is described in Sect. 8, and starting and finishing procedures are discussed in Sect. 9. The results of some numerical experiments with these methods are reported in Sect. 10. Finally, some concluding remarks and plans for future research are presented in Sect. 11.

## 2 Partitioned GLMs and IMEX Schemes

For the numerical solution of (1), we consider the partitioned method, where the first and the second subsystems of (1) are integrated by the explicit and diagonally implicit GLMs, respectively. These methods on the uniform grid

$$t_i = t_0 + ih, \quad i = 0, 1, \dots, N, \quad Nh = t_{\text{end}} - t_0$$

are defined by

$$\begin{cases} X_i^{[n+1]} = h \sum_{j=1}^{i-1} a_{ij} f(X_j^{[n+1]}, Z_j^{[n+1]}) + \sum_{j=1}^r u_{ij} x_j^{[n]}, & i = 1, 2, \dots, s, \\ x_i^{[n+1]} = h \sum_{j=1}^s b_{ij} f(X_j^{[n+1]}, Z_j^{[n+1]}) + \sum_{j=1}^r v_{ij} x_j^{[n]}, & i = 1, 2, \dots, r, \end{cases} \quad (3)$$

$n = 0, 1, \dots, N - 1$ , and

$$\begin{cases} Z_i^{[n+1]} = h \sum_{j=1}^i \hat{a}_{ij} g(X_j^{[n+1]}, Z_j^{[n+1]}) + \sum_{j=1}^r \hat{u}_{ij} z_j^{[n]}, & i = 1, 2, \dots, s, \\ z_i^{[n+1]} = h \sum_{j=1}^s \hat{b}_{ij} g(X_j^{[n+1]}, Z_j^{[n+1]}) + \sum_{j=1}^r \hat{v}_{ij} z_j^{[n]}, & i = 1, 2, \dots, r, \end{cases} \tag{4}$$

$n = 0, 1, \dots, N - 1$ . We assume that the components of the input vectors  $x^{[n-1]}$  and  $z^{[n-1]}$  for the next step satisfy the relations

$$x_i^{[n-1]} = \sum_{k=0}^q q_{ik} h^k x^{(k)}(t_{n-1}) + O(h^{p+1}), \quad z_i^{[n-1]} = \sum_{k=0}^q \hat{q}_{ik} h^k z^{(k)}(t_{n-1}) + O(h^{p+1}),$$

$i = 1, 2, \dots, r$ , for some constants  $q_{ik}$  and  $\hat{q}_{ik}$ , and request that

$$X_i^{[n+1]} = x(t_n + c_i h) + O(h^{q+1}), \quad Z_i^{[n+1]} = z(t_n + \hat{c}_i h) + O(h^{q+1}), \tag{5}$$

$i = 1, 2, \dots, s$ , and

$$x_i^{[n]} = \sum_{k=0}^q q_{ik} h^k x^{(k)}(t_n) + O(h^{p+1}), \quad z_i^{[n]} = \sum_{k=0}^q \hat{q}_{ik} h^k z^{(k)}(t_n) + O(h^{p+1}), \tag{6}$$

$i = 1, 2, \dots, r$ , for the same constants  $q_{ik}$  and  $\hat{q}_{ik}$ . The explicit method (3) is characterized by the abscissa vector  $c = [c_1, \dots, c_s]^T \in \mathbb{R}^s$ , four coefficient matrices

$$A = [a_{ij}] \in \mathbb{R}^{s \times s}, \quad U = [u_{ij}] \in \mathbb{R}^{s \times r}, \quad B = [b_{ij}] \in \mathbb{R}^{r \times s}, \quad V = [v_{ij}] \in \mathbb{R}^{r \times r},$$

and the vectors

$$q_k = [q_{1,k} \ q_{2,k} \ \dots \ q_{r,k}]^T \in \mathbb{R}^r, \quad k = 1, 2, \dots, q.$$

Similarly, the implicit method (4) is characterized by the abscissa vector  $\hat{c} = [\hat{c}_1, \dots, \hat{c}_s]^T \in \mathbb{R}^s$ , four coefficient matrices

$$\hat{A} = [\hat{a}_{ij}] \in \mathbb{R}^{s \times s}, \quad \hat{U} = [\hat{u}_{ij}] \in \mathbb{R}^{s \times r}, \quad \hat{B} = [\hat{b}_{ij}] \in \mathbb{R}^{r \times s}, \quad \hat{V} = [\hat{v}_{ij}] \in \mathbb{R}^{r \times r},$$

and the vectors

$$\hat{q}_k = [\hat{q}_{1,k} \ \hat{q}_{2,k} \ \dots \ \hat{q}_{r,k}]^T \in \mathbb{R}^r, \quad k = 1, 2, \dots, q.$$

These methods are also characterized by four integers  $p, q, r$ , and  $s$ , where  $p$  is the order,  $q$  the stage order,  $r$  the number of external approximations, and  $s$  the number of internal approximations or stages.

Introducing the notation

$$\begin{aligned}
 X^{[n+1]} &= \begin{bmatrix} X_1^{[n+1]} \\ \vdots \\ X_s^{[n+1]} \end{bmatrix}, \quad x^{[n]} = \begin{bmatrix} x_1^{[n]} \\ \vdots \\ x_r^{[n]} \end{bmatrix}, \quad x(t_n + ch) = \begin{bmatrix} x(t_n + c_1 h) \\ \vdots \\ x(t_n + c_s h) \end{bmatrix}, \\
 f(X^{[n+1]}, Z^{[n+1]}) &= \begin{bmatrix} f(X_1^{[n+1]}, Z_1^{[n+1]}) \\ \vdots \\ f(X_s^{[n+1]}, Z_s^{[n+1]}) \end{bmatrix}, \\
 Z^{[n+1]} &= \begin{bmatrix} Z_1^{[n+1]} \\ \vdots \\ Z_s^{[n+1]} \end{bmatrix}, \quad z^{[n]} = \begin{bmatrix} z_1^{[n]} \\ \vdots \\ z_r^{[n]} \end{bmatrix}, \quad z(t_n + \hat{c}h) = \begin{bmatrix} z(t_n + \hat{c}_1 h) \\ \vdots \\ z(t_n + \hat{c}_s h) \end{bmatrix}, \\
 g(X^{[n+1]}, Z^{[n+1]}) &= \begin{bmatrix} g(X_1^{[n+1]}, Z_1^{[n+1]}) \\ \vdots \\ g(X_s^{[n+1]}, Z_s^{[n+1]}) \end{bmatrix},
 \end{aligned}$$

the methods (3) and (4) can be written in the vector form

$$\begin{cases} X^{[n+1]} = h(A \otimes I)f(X^{[n+1]}, Z^{[n+1]}) + (U \otimes I)x^{[n]}, \\ x^{[n+1]} = h(B \otimes I)f(X^{[n+1]}, Z^{[n+1]}) + (V \otimes I)x^{[n]}, \end{cases} \quad (7)$$

$n = 0, 1, \dots, N - 1$ , and

$$\begin{cases} Z^{[n+1]} = h(\hat{A} \otimes \hat{I})g(X^{[n+1]}, Z^{[n+1]}) + (\hat{U} \otimes \hat{I})z^{[n]}, \\ z^{[n+1]} = h(\hat{B} \otimes \hat{I})g(X^{[n+1]}, Z^{[n+1]}) + (\hat{V} \otimes \hat{I})z^{[n]}, \end{cases} \quad (8)$$

$n = 0, 1, \dots, N - 1$ . Here,  $I$  is the identity matrix of dimension  $m$ , and  $\hat{I}$  is the identity matrix of dimension  $n$ . The relations (5) and (6) take now the form

$$X^{[n+1]} = x(t_n + ch) + O(h^{q+1}), \quad Z^{[n+1]} = z(t_n + \hat{c}h) + O(h^{q+1}), \quad (9)$$

and

$$x^{[n]} = \sum_{k=0}^q (q_k \otimes I)h^k x^{(k)}(t_n) + O(h^{p+1}), \quad z^{[n]} = \sum_{k=0}^q (\hat{q}_k \otimes \hat{I})h^k z^{(k)}(t_n) + O(h^{p+1}). \quad (10)$$

We will reformulate next the methods (7) and (8) as GLM for the system (2). To simplify this reformulation, as well as the theoretical analysis of order and stage order conditions which is undertaken in the next section, and SSP properties discussed in Sects. 5 and 7, we will assume that the number of equations  $m$  of the nonstiff subsystem of (1) is equal to the number of equations  $n$  of the stiff subsystem. This assumption can be made without loss of generality, since if this is not the case, the subsystem with smaller number of equations can be padded by adding the equations of the form  $y_v'(t) = 0$ ,  $y_v(t_0) = 0$ , or repeating some of the equations of this subsystem. Putting

$$\begin{aligned}
 Y^{[n+1]} &= \begin{bmatrix} X^{[n+1]} \\ Z^{[n+1]} \end{bmatrix}, \quad y^{[n]} = \begin{bmatrix} x^{[n]} \\ z^{[n]} \end{bmatrix}, \\
 F(Y^{[n+1]}) &= \begin{bmatrix} f(X^{[n+1]}, Z^{[n+1]}) \\ g(X^{[n+1]}, Z^{[n+1]}) \end{bmatrix} = \begin{bmatrix} f(Y^{[n+1]}) \\ g(Y^{[n+1]}) \end{bmatrix},
 \end{aligned}$$

and taking into account that for any matrices  $Q$  and  $\hat{Q}$ , we have

$$\begin{bmatrix} Q \otimes I & 0 \\ 0 & \hat{Q} \otimes I \end{bmatrix} = \begin{bmatrix} Q & 0 \\ 0 & \hat{Q} \end{bmatrix} \otimes \mathbf{I},$$

where  $I$  and  $\mathbf{I}$  stand for identity matrices of dimension  $m$ , leads to

$$\begin{cases} Y^{[n+1]} = h(\mathbf{A} \otimes \mathbf{I})F(Y^{[n+1]}) + (\mathbf{U} \otimes \mathbf{I})y^{[n]}, \\ y^{[n+1]} = h(\mathbf{B} \otimes \mathbf{I})F(Y^{[n+1]}) + (\mathbf{V} \otimes \mathbf{I})y^{[n]}, \end{cases} \tag{11}$$

$n = 0, 1, \dots, N - 1$ . Here, the abscissa vector  $\mathbf{c}$  and the coefficient matrices  $\mathbf{A}$ ,  $\mathbf{U}$ ,  $\mathbf{B}$ , and  $\mathbf{V}$  are defined by

$$\begin{aligned} \mathbf{c} &= \begin{bmatrix} c \\ \hat{c} \end{bmatrix} \in \mathbb{R}^{2s}, \quad \mathbf{A} = \begin{bmatrix} A & 0 \\ 0 & \hat{A} \end{bmatrix} \in \mathbb{R}^{2s \times 2s}, \quad \mathbf{U} = \begin{bmatrix} U & 0 \\ 0 & \hat{U} \end{bmatrix} \in \mathbb{R}^{2s \times 2r}, \\ \mathbf{B} &= \begin{bmatrix} B & 0 \\ 0 & \hat{B} \end{bmatrix} \in \mathbb{R}^{2r \times 2s}, \quad \mathbf{V} = \begin{bmatrix} V & 0 \\ 0 & \hat{V} \end{bmatrix} \in \mathbb{R}^{2r \times 2r}. \end{aligned} \tag{12}$$

Observe that for this method, the relations (9) and (10) assume the form

$$Y^{[n+1]} = y(t_n + \mathbf{c}h) + O(h^{p+1}), \tag{13}$$

and

$$y^{[n]} = \sum_{k=0}^q (\mathbf{q}_k \otimes \mathbf{I})h^k y^{(k)}(t_n) + O(h^{q+1}), \tag{14}$$

where  $\mathbf{q}_k$  are now matrices defined by

$$\mathbf{q}_k = \begin{bmatrix} q_k & 0 \\ 0 & \hat{q}_k \end{bmatrix} \in \mathbb{R}^{2r \times 2}, \quad k = 0, 1, \dots, q. \tag{15}$$

### 3 Stage Order and Order Conditions

In the remainder of the paper, we will be concerned with GLMs (11) of order  $p$  and stage order  $q = p$ . As in [49] it will be always assumed that the partitioned GLMs (7) and (8) are internally consistent, i.e., they have the same abscissa vectors  $c = \hat{c}$ . This condition implies that all stage components  $X_i^{[n+1]}$  and  $Z_i^{[n+1]}$  approximate the solutions  $x$  and  $z$  to (1) at the same time points  $t_n + c_i h, i = 1, 2, \dots, s$ .

To derive order conditions for such methods, we consider local discretization errors  $\eta(t_n, h)$  and  $\xi(t_n, h)$  of internal and external stages of (11), which are defined by the relations

$$\begin{aligned} \eta(t_n, h) &= y(t_n + \mathbf{c}h) - h(\mathbf{A} \otimes \mathbf{I})F(y(t_n + \mathbf{c}h)) \\ &\quad - (\mathbf{U} \otimes \mathbf{I}) \sum_{k=0}^p (\mathbf{q}_k \otimes \mathbf{I})h^k y^{(k)}(t_n), \end{aligned} \tag{16}$$

and

$$\begin{aligned} \xi(t_n, h) &= \sum_{k=0}^p (\mathbf{q}_k \otimes \mathbf{I}) h^k y^{(k)}(t_{n+1}) - h(\mathbf{B} \otimes \mathbf{I})F(y(t_n + \mathbf{c}h)) \\ &\quad - (\mathbf{V} \otimes \mathbf{I}) \sum_{k=0}^p (\mathbf{q}_k \otimes \mathbf{I}) h^k y^{(k)}(t_n), \end{aligned} \tag{17}$$

$n = 0, 1, \dots, N - 1$ . Here,

$$y(t_n + \mathbf{c}h) = \begin{bmatrix} x(t_n + ch) \\ z(t_n + ch) \end{bmatrix},$$

and  $x(t_n + ch)$  and  $z(t_n + ch)$  are defined in Sect. 2. Then, the method (11) has order  $p$  and stage order  $q = p$  if and only if

$$\eta(t_n, h) = O(h^{p+1}) \quad \text{and} \quad \xi(t_n, h) = O(h^{p+1}) \quad \text{as} \quad h \rightarrow 0.$$

We have the following theorem.

**Theorem 1** *The internally consistent GLM (11) defined by abscissa vector  $\mathbf{c}$  with  $c = \hat{c}$ , and coefficient matrices  $\mathbf{A}, \mathbf{U}, \mathbf{B}, \mathbf{V}$  given by (12), and the matrices  $\mathbf{q}_k, k = 0, 1, \dots, p$ , given by (15), has order  $p$  and stage order  $q = p$  if and only if the explicit GLM defined by  $c, A, U, B, V$ , and  $q_k, k = 0, 1, \dots, p$ , and implicit GLM defined by  $c, \hat{A}, \hat{U}, \hat{B}, \hat{V}$ , and  $\hat{q}_k, k = 0, 1, \dots, p$ , have order  $p$  and stage order  $q = p$ .*

**Proof** Let us partition the vectors  $\eta(t_n, h)$  and  $\xi(t_n, h)$  as

$$\eta(t_n, h) = \begin{bmatrix} \eta_E(t_n, h) \\ \eta_I(t_n, h) \end{bmatrix}, \quad \xi(t_n, h) = \begin{bmatrix} \xi_E(t_n, h) \\ \xi_I(t_n, h) \end{bmatrix},$$

where  $\eta_E(t_n, h), \xi_E(t_n, h)$  correspond to the first  $m$  non-stiff components of  $\eta(t_n, h), \xi(t_n, h)$ , and  $\eta_I(t_n, h), \xi_I(t_n, h)$  correspond to the last  $n$  stiff components of  $\eta(t_n, h), \xi(t_n, h)$ . Then, taking into account that  $y'(t_n + \mathbf{c}h) = F(y(t_n + \mathbf{c}h))$ , we obtain

$$\begin{aligned} \begin{bmatrix} \eta_E(t_n, h) \\ \eta_I(t_n, h) \end{bmatrix} &= \begin{bmatrix} x(t_n + ch) \\ z(t_n + ch) \end{bmatrix} - h \begin{bmatrix} A \otimes I & 0 \\ 0 & \hat{A} \otimes \hat{I} \end{bmatrix} \begin{bmatrix} x'(t_n + ch) \\ z'(t_n + ch) \end{bmatrix} \\ &\quad - \sum_{k=0}^p \begin{bmatrix} U \otimes I & 0 \\ 0 & \hat{U} \otimes \hat{I} \end{bmatrix} \begin{bmatrix} q_k \otimes I & 0 \\ 0 & \hat{q}_k \otimes \hat{I} \end{bmatrix} h^k \begin{bmatrix} x^{(k)}(t_n) \\ z^{(k)}(t_n) \end{bmatrix}, \end{aligned}$$

and

$$\begin{aligned} \begin{bmatrix} \xi_E(t_n, h) \\ \xi_I(t_n, h) \end{bmatrix} &= \sum_{k=0}^p \begin{bmatrix} q_k \otimes I & 0 \\ 0 & \hat{q}_k \otimes \hat{I} \end{bmatrix} h^k \begin{bmatrix} x^{(k)}(t_{n+1}) \\ z^{(k)}(t_{n+1}) \end{bmatrix} \\ &\quad - h \begin{bmatrix} B \otimes I & 0 \\ 0 & \hat{B} \otimes \hat{I} \end{bmatrix} \begin{bmatrix} x'(t_n + ch) \\ z'(t_n + ch) \end{bmatrix} \\ &\quad - \sum_{k=0}^p \begin{bmatrix} V \otimes I & 0 \\ 0 & \hat{V} \otimes \hat{I} \end{bmatrix} \begin{bmatrix} q_k \otimes I & 0 \\ 0 & \hat{q}_k \otimes \hat{I} \end{bmatrix} h^k \begin{bmatrix} x^{(k)}(t_n) \\ z^{(k)}(t_n) \end{bmatrix}. \end{aligned}$$

These relations imply that

$$\eta_E(t_n, h) = x(t_n + ch) - h(A \otimes I)x'(t_n + ch) - \sum_{k=0}^p (Vq_k \otimes I)h^k x^{(k)}(t_n),$$

$$\xi_E(t_n, h) = \sum_{k=0}^p (q_k \otimes I)h^k x^{(k)}(t_{n+1}) - h(B \otimes I)x'(t_n + ch) - \sum_{k=0}^p (Vq_k \otimes I)h^k x^{(k)}(t_n),$$

and

$$\eta_I(t_n, h) = z(t_n + ch) - h(\widehat{A} \otimes I)z'(t_n + ch) - \sum_{k=0}^p (\widehat{V}\widehat{q}_k \otimes I)h^k z^{(k)}(t_n),$$

$$\xi_I(t_n, h) = \sum_{k=0}^p (\widehat{q}_k \otimes I)h^k z^{(k)}(t_{n+1}) - h(\widehat{B} \otimes I)z'(t_n + ch) - \sum_{k=0}^p (\widehat{V}\widehat{q}_k \otimes I)h^k z^{(k)}(t_n).$$

We recognize  $\eta_E(t_n, h)$  and  $\xi_E(t_n, h)$  as local discretization errors of internal and external stages of explicit GLM (7), and  $\eta_I(t_n, h)$  and  $\xi_I(t_n, h)$  as local discretization errors of internal and external stages of implicit GLM (8). Hence, the explicit and implicit methods (7) and (8) have order  $p$  and stage order  $q = p$ , i.e.,

$$\eta_E(t_n, h) = O(h^{p+1}) \quad \text{and} \quad \xi_E(t_n, h) = O(h^{p+1}) \quad \text{as} \quad h \rightarrow 0,$$

and

$$\eta_I(t_n, h) = O(h^{p+1}) \quad \text{and} \quad \xi_I(t_n, h) = O(h^{p+1}) \quad \text{as} \quad h \rightarrow 0,$$

if and only if the IMEX scheme (11) has order  $p$  and stage order  $q = p$ , i.e.,

$$\eta(t_n, h) = O(h^{p+1}) \quad \text{and} \quad \xi(t_n, h) = O(h^{p+1}) \quad \text{as} \quad h \rightarrow 0.$$

These arguments complete the proof.

We can derive stage order and order conditions for explicit and implicit GLMs (7) and (8) by expanding  $x(t_n + ch)$ ,  $x'(t_n + ch)$ ,  $x^{(k)}(t_{n+1})$ , and  $z(t_n + ch)$ ,  $z'(t_n + ch)$ ,  $z^{(k)}(t_{n+1})$ , appearing in  $\eta_E(t_n, h)$ ,  $\xi_E(t_n, h)$ , and  $\eta_I(t_n, h)$ ,  $\xi_I(t_n, h)$ , into Taylor series around  $t_n$ , and comparing to zero the terms with powers  $h^k$ ,  $k = 0, 1, \dots, p$ . Such stage order and order conditions were derived in [3, 4] and in the monograph [36]. To make this paper self-contained, these stage order and order conditions are also listed in Theorem 2 below.

**Theorem 2** *The GLMs (7) and (8) have order  $p$  and stage order  $q = p$  if and only if*

$$\frac{c^k}{k!} - \frac{A c^{k-1}}{(k-1)!} - Uq_k = 0, \quad k = 0, 1, \dots, p, \tag{18}$$

$$\sum_{l=0}^k \frac{1}{l!} q_{k-l} - \frac{B c^{k-1}}{(k-1)!} - Vq_k = 0, \quad k = 0, 1, \dots, p, \tag{19}$$

and

$$\frac{c^k}{k!} - \frac{\widehat{A} c^{k-1}}{(k-1)!} - \widehat{U}\widehat{q}_k = 0, \quad k = 0, 1, \dots, p, \tag{20}$$

$$\sum_{l=0}^k \frac{1}{l!} \hat{q}_{k-l} - \frac{\hat{B}c^{k-1}}{(k-1)!} - \hat{V} \hat{q}_k = 0, \quad k = 0, 1, \dots, p. \quad (21)$$

For  $k = 0$ , we obtain the pre-consistency conditions

$$Uq_0 = e, \quad Vq_0 = q_0, \quad \hat{U}\hat{q}_0 = e, \quad \hat{V}\hat{q}_0 = \hat{q}_0,$$

where  $e = [1, \dots, 1]^T \in \mathbb{R}^r$ . For the methods investigated in this paper, the pre-consistency vectors  $q_0$  and  $\hat{q}_0$  are given by

$$q_0 = \hat{q}_0 = [1 \ 0 \ \dots \ 0] \in \mathbb{R}^r.$$

It follows from Theorem 1 that the IMEX scheme (11) has order  $p$  and stage order  $q = p$  if the “component” GLMs (7) and (8) independently meet the conditions (18), (19), (20), and (21), for order  $p$  and stage order  $q = p$ . Contrary to partitioned Runge-Kutta methods, considered for example in [21], no coupling conditions are required, i.e., conditions involving parameters of both methods. This result was also proved, using somewhat different arguments, in [49], for internally consistent partitioned GLMs of order  $p$  and stage order  $q = p$  or  $q = p - 1$ .

#### 4 Stability Properties of IMEX Schemes

We consider first the decoupled linear test system

$$\begin{cases} x'(t) = \lambda x(t), \\ z'(t) = \lambda z(t), \end{cases} \quad (22)$$

$t \geq 0$ , where  $\lambda$  is a complex parameter. Then applying IMEX scheme (11) to this system the first equation of (22) is treated by the explicit GLM with abscissa vector  $c$  and coefficient matrices  $A$ ,  $U$ ,  $B$ ,  $V$ , and the second equation of (22) is treated by the implicit GLM with the same abscissa vector  $c$  and coefficient matrices  $\hat{A}$ ,  $\hat{U}$ ,  $\hat{B}$ ,  $\hat{V}$ . This leads to the relations

$$x^{[n+1]} = M_E(z) x^{[n]},$$

$n = 0, 1, \dots$ ,  $z = h\lambda$ , with stability matrix  $M_E(z)$  given by

$$M_E(z) = V + zB(I - zA)^{-1}U,$$

and

$$z^{[n+1]} = M_I(z) z^{[n]},$$

$n = 0, 1, \dots$ ,  $z = h\lambda$ , with stability matrix  $M_I(z)$  given by

$$M_I(z) = \hat{V} + z\hat{B}(I - z\hat{A})^{-1}\hat{U}.$$

Hence, it follows that the absolute stability properties of IMEX method with respect to (22) are combinations of absolute stability properties of explicit and implicit parts of the scheme. In this paper we will search for IMEX schemes, where the explicit and implicit GLMs have so-called inherent Runge-Kutta stability (IRKS) [5, 36, 47, 48], and the



implicit GLM is  $A$ - and  $L$ -stable. Moreover, we will monitor the size of the region of absolute stability of the explicit GLM.

We consider next the coupled linear test system of the form

$$\begin{cases} x'(t) = ax(t) + bz(t), \\ z'(t) = bx(t) + az(t), \end{cases} \tag{23}$$

$t \geq 0$ , where  $a$  and  $b$  are real parameters. The solutions  $(x(t), z(t))$  tend to zero as  $t$  tends to the infinity if and only if

$$a - b < 0, \quad a + b < 0,$$

and we will investigate whether this property is inherited by the numerical approximations  $(x^{[n]}, z^{[n]})$  obtained by application of IMEX method (11) to the system (23).

Applying (11) to (23) we obtain

$$\begin{bmatrix} X^{[n+1]} \\ Z^{[n+1]} \end{bmatrix} = h \begin{bmatrix} A & 0 \\ 0 & \hat{A} \end{bmatrix} \begin{bmatrix} aX^{[n+1]} + bZ^{[n+1]} \\ bX^{[n+1]} + aZ^{[n+1]} \end{bmatrix} + \begin{bmatrix} U & 0 \\ 0 & \hat{U} \end{bmatrix} \begin{bmatrix} x^{[n]} \\ z^{[n]} \end{bmatrix},$$

and

$$\begin{bmatrix} x^{[n+1]} \\ z^{[n+1]} \end{bmatrix} = h \begin{bmatrix} B & 0 \\ 0 & \hat{B} \end{bmatrix} \begin{bmatrix} aX^{[n+1]} + bZ^{[n+1]} \\ bX^{[n+1]} + aZ^{[n+1]} \end{bmatrix} + \begin{bmatrix} V & 0 \\ 0 & \hat{V} \end{bmatrix} \begin{bmatrix} x^{[n]} \\ z^{[n]} \end{bmatrix},$$

$n = 0, 1, \dots$ . These equations can be rewritten in the form

$$\begin{bmatrix} X^{[n+1]} \\ Z^{[n+1]} \end{bmatrix} = \begin{bmatrix} \alpha A & \beta A \\ \beta \hat{A} & \alpha \hat{A} \end{bmatrix} \begin{bmatrix} X^{[n+1]} \\ Z^{[n+1]} \end{bmatrix} + \begin{bmatrix} U & 0 \\ 0 & \hat{U} \end{bmatrix} \begin{bmatrix} x^{[n]} \\ z^{[n]} \end{bmatrix}, \tag{24}$$

and

$$\begin{bmatrix} x^{[n+1]} \\ z^{[n+1]} \end{bmatrix} = \begin{bmatrix} \alpha B & \beta B \\ \beta \hat{B} & \alpha \hat{B} \end{bmatrix} \begin{bmatrix} X^{[n+1]} \\ Z^{[n+1]} \end{bmatrix} + \begin{bmatrix} V & 0 \\ 0 & \hat{V} \end{bmatrix} \begin{bmatrix} x^{[n]} \\ z^{[n]} \end{bmatrix}, \tag{25}$$

$n = 0, 1, \dots$ , where  $\alpha = ha$  and  $\beta = hb$ . Solving the equation (24) with respect to the vector of stage values, we obtain

$$\begin{bmatrix} X^{[n+1]} \\ Z^{[n+1]} \end{bmatrix} = \begin{bmatrix} I - \alpha A & -\beta A \\ -\beta \hat{A} & I - \alpha \hat{A} \end{bmatrix}^{-1} \begin{bmatrix} U & 0 \\ 0 & \hat{U} \end{bmatrix} \begin{bmatrix} x^{[n]} \\ z^{[n]} \end{bmatrix}.$$

Substituting the above relation into (25) leads to the vector recurrence equation

$$\begin{bmatrix} x^{[n+1]} \\ z^{[n+1]} \end{bmatrix} = \mathbf{M}_{\text{IMEX}}(\alpha, \beta) \begin{bmatrix} x^{[n]} \\ z^{[n]} \end{bmatrix}, \tag{26}$$

$n = 0, 1, \dots$ , with stability matrix  $\mathbf{M}_{\text{IMEX}}(\alpha, \beta)$  of IMEX scheme defined by

$$\mathbf{M}_{\text{IMEX}}(\alpha, \beta) = \begin{bmatrix} V & 0 \\ 0 & \hat{V} \end{bmatrix} + \begin{bmatrix} \alpha B & \beta B \\ \beta \hat{B} & \alpha \hat{B} \end{bmatrix} \begin{bmatrix} I - \alpha A & -\beta A \\ -\beta \hat{A} & I - \alpha \hat{A} \end{bmatrix}^{-1} \begin{bmatrix} U & 0 \\ 0 & \hat{U} \end{bmatrix}. \tag{27}$$

Observe that for  $\beta = 0$  we have

$$\begin{aligned} \mathbf{M}_{\text{IMEX}}(\alpha, 0) &= \begin{bmatrix} V & 0 \\ 0 & \widehat{V} \end{bmatrix} + \begin{bmatrix} \alpha B & 0 \\ 0 & \alpha \widehat{B} \end{bmatrix} \begin{bmatrix} I - \alpha A & 0 \\ 0 & I - \alpha \widehat{A} \end{bmatrix}^{-1} \begin{bmatrix} U & 0 \\ 0 & \widehat{U} \end{bmatrix} \\ &= \begin{bmatrix} V + \alpha B(I - \alpha A)^{-1}U & 0 \\ 0 & \widehat{V} + \alpha \widehat{B}(I - \alpha \widehat{A})^{-1}\widehat{U} \end{bmatrix} \\ &= \begin{bmatrix} M_E(\alpha) & 0 \\ 0 & M_I(\alpha) \end{bmatrix}, \end{aligned}$$

where  $M_E(\alpha)$  and  $M_I(\alpha)$  are stability functions of explicit and implicit GLMs, respectively, with respect to (22) corresponding to  $\text{Re}(z) = \alpha$ . We also define stability polynomial  $\mathbf{p}_{\text{IMEX}}(w; \alpha, \beta)$  with respect to the test system (23) by the relation

$$\mathbf{p}_{\text{IMEX}}(w; \alpha, \beta) = \det(w\mathbf{I} - \mathbf{M}_{\text{IMEX}}(\alpha, \beta)), \quad (28)$$

and the stability region with respect to (23) is then given by

$$\mathcal{A}_{\text{IMEX}} = \left\{ (\alpha, \beta) : \mathbf{p}_{\text{IMEX}}(w; \alpha, \beta) \text{ is a Schur polynomial} \right\}. \quad (29)$$

We recall that  $\mathbf{p}_{\text{IMEX}}(w; \alpha, \beta)$  is a Schur polynomial if all its roots  $w_i$ ,  $i = 1, 2, \dots, 2s$ , are inside of the unit circle. Stability regions  $\mathcal{A}_{\text{IMEX}}$  defined by (29), with respect to the test system (23), for SSP IMEX GLMs of order  $p = 1, 2, 3$ , and 4, and stage order  $q = p$ , are displayed in Sect. 8.

## 5 SSP Property of IMEX GLMs

Since IMEX methods for (1) can be reformulated as GLMs for (2), we can define SSP property of IMEX schemes in the same way this was done for GLMs. To define this SSP property of IMEX schemes (11), we assume that the discretization of the initial-value problem (2) by the forward Euler method

$$y_{n+1} = y_n + h_{FE}F(y_n), \quad y_0 = y(t_0),$$

$n = 0, 1, \dots, N - 1$ , is monotone or contractive. This means that the inequality

$$\|y_{n+1}\| \leq \|y_n\| \quad (30)$$

is satisfied for all  $n = 0, 1, \dots, N - 1$ , in some norm or semi-norm  $\|\cdot\|$ , under the following restriction on the stepsize  $h$  of integration

$$h \leq h_{FE}. \quad (31)$$

Following Spijker [44], we will say that the GLM (11) is monotone or contractive if

$$\|Y^{[n+1]}\| \leq \|y^{[n+1]}\| \quad (32)$$

for  $n = 0, 1, \dots, N - 1$ , under the modified step size restriction

$$h \leq \mathcal{C} \cdot h_{FE}, \quad (33)$$

where  $Y^{[n+1]}$  and  $y^{[n+1]}$  are defined by (11). IMEX schemes for (2) that satisfy the monotonicity condition (32) under the step size restriction (33) with  $\mathcal{C} > 0$  are said to have the SSP property, and the maximal constant  $\mathcal{C}$  in (33) is called the SSP coefficient. As in [7, 10, 39],

to compare methods with different number of internal stages  $s$ , we also define the effective SSP coefficient  $C_{\text{eff}}$  by the formula

$$C_{\text{eff}} = C/s. \tag{34}$$

Runge-Kutta and linear multistep methods with SSP property have been studied by Shu and Osher [43], Gottlieb et al. [20], Spiteri and Ruuth [45], Hundsdorfer et al. [30], Gottlieb [16], Hundsdorfer and Ruuth [28], Ruuth and Hundsdorfer [41], Gottlieb and Ruuth [19], Gottlieb et al. [17, 18], Higuera [23–25], and Ferracina and Spijker [12–15]. Two-step Runge-Kutta methods, proposed in [36, 37], with the SSP property were investigated by Ketcheson et al. [39], and SSP multistep multistage schemes were investigated by Constantinescu and Sandu [10]. SSP GLMs were investigated by Spijker in his seminal work [44], by Izzo and Jackiewicz [31, 32, 34, 35], and by Califano et al. [7], using the results from [44]. Also in this paper we will employ Spijker [44] results to construct internally consistent SSP IMEX GLMs up to the order  $p = 4$  and stage order  $q = p$ .

The characterization of SSP IMEX methods is investigated in Sect. 7 for the large class of IMEX transformed GLMs (TGLMs) defined in Sect. 6

### 6 IMEX TGLMs

Similarly as in [34, 35], a class of IMEX TGLMs is defined by multiplying the relation for  $y^{[n+1]}$  in (11) by the transformation matrix  $\mathbf{T} \otimes \mathbf{I}$ , where

$$\mathbf{T} = \begin{bmatrix} T & 0 \\ 0 & \hat{T} \end{bmatrix} \in \mathbb{R}^{2r \times 2r}, \quad T, \hat{T} \in \mathbb{R}^{r \times r},$$

and  $\det(T) \neq 0, \det(\hat{T}) \neq 0$ . This leads to

$$\begin{cases} Y^{[n+1]} = h(\mathbf{A} \otimes \mathbf{I})F(Y^{[n+1]}) + (\mathbf{U} \otimes \mathbf{I})(\mathbf{T}^{-1} \otimes \mathbf{I})(\mathbf{T} \otimes \mathbf{I})y^{[n]}, \\ (\mathbf{T} \otimes \mathbf{I})y^{[n+1]} = h(\mathbf{T} \otimes \mathbf{I})(\mathbf{B} \otimes \mathbf{I})F(Y^{[n+1]}) \\ \quad + (\mathbf{T} \otimes \mathbf{I})(\mathbf{V} \otimes \mathbf{I})(\mathbf{T}^{-1} \otimes \mathbf{I})(\mathbf{T} \otimes \mathbf{I})y^{[n]}, \end{cases} \tag{35}$$

$n = 0, 1, \dots, N - 1$ . Define the transformed vectors of external approximations by

$$\bar{y}^{[n+1]} = (\mathbf{T} \otimes \mathbf{I})y^{[n+1]}, \quad \bar{y}^{[n]} = (\mathbf{T} \otimes \mathbf{I})y^{[n]},$$

and the transformed coefficient matrices by

$$\mathbf{A}^* = \mathbf{A}, \quad \mathbf{U}^* = \mathbf{U}\mathbf{T}^{-1}, \quad \mathbf{B}^* = \mathbf{T}\mathbf{B}, \quad \mathbf{V}^* = \mathbf{T}\mathbf{V}\mathbf{T}^{-1}, \quad \mathbf{q}_k^* = \mathbf{T}\mathbf{q}_k, \quad k = 0, 1, \dots, p.$$

Observe that these matrices have the following block structure:

$$\begin{aligned}
 \mathbf{A}^* &= \begin{bmatrix} A^* & 0 \\ 0 & \hat{A}^* \end{bmatrix}, & A^* &= A, & \hat{A}^* &= \hat{A}, \\
 \mathbf{U}^* &= \begin{bmatrix} U^* & 0 \\ 0 & \hat{U}^* \end{bmatrix}, & U^* &= UT^{-1}, & \hat{U}^* &= \hat{U}\hat{T}^{-1}, \\
 \mathbf{B}^* &= \begin{bmatrix} B^* & 0 \\ 0 & \hat{B}^* \end{bmatrix}, & B^* &= TB, & \hat{B}^* &= \hat{T}\hat{B}, \\
 \mathbf{V}^* &= \begin{bmatrix} V^* & 0 \\ 0 & \hat{V}^* \end{bmatrix}, & V^* &= TVT^{-1}, & \hat{V}^* &= \hat{T}\hat{V}\hat{T}^{-1}, \\
 \mathbf{q}_k^* &= \begin{bmatrix} Tq_k & 0 \\ 0 & \hat{T}\hat{q}_k \end{bmatrix}, & & & k &= 0, 1, \dots, p.
 \end{aligned}$$

Then the method (35) can be rewritten in the following form:

$$\begin{cases} Y^{[n+1]} = h(\mathbf{A}^* \otimes \mathbf{I})F(Y^{[n+1]}) + (\mathbf{U}^* \otimes \mathbf{I})\bar{y}^{[n]}, \\ \bar{y}^{[n+1]} = h(\mathbf{B}^* \otimes \mathbf{I})F(Y^{[n+1]}) + (\mathbf{V}^* \otimes \mathbf{I})\bar{y}^{[n]}, \end{cases} \tag{36}$$

$n = 0, 1, \dots, N - 1$ .

Similarly as in [34, 35], we can show that the IMEX TGLMs (36) preserve the order and stage order of the original methods (11), and have the same stability properties with respect to the basic test system (22).

To investigate stability properties of IMEX TGLMs with respect to the test system (23), we examine the stability matrix  $\mathbf{M}_{\text{IMEX}}^*(\alpha, \beta)$  corresponding to this scheme. We have

$$\begin{aligned}
 \mathbf{M}_{\text{IMEX}}^*(\alpha, \beta) &= \begin{bmatrix} V^* & 0 \\ 0 & \hat{V}^* \end{bmatrix} \\
 &+ \begin{bmatrix} \alpha B^* & \beta B^* \\ \beta \hat{B}^* & \alpha \hat{B}^* \end{bmatrix} \begin{bmatrix} I - \alpha A^* & -\beta A^* \\ -\beta \hat{A}^* & I - \alpha \hat{A}^* \end{bmatrix}^{-1} \begin{bmatrix} U^* & 0 \\ 0 & \hat{U}^* \end{bmatrix} \\
 &= \begin{bmatrix} TVT^{-1} & 0 \\ 0 & \hat{T}\hat{V}\hat{T}^{-1} \end{bmatrix} \\
 &+ \begin{bmatrix} \alpha TB & \beta TB \\ \beta \hat{T}\hat{B} & \alpha \hat{T}\hat{B} \end{bmatrix} \begin{bmatrix} I - \alpha A & -\beta A \\ -\beta \hat{A} & I - \alpha \hat{A} \end{bmatrix}^{-1} \begin{bmatrix} UT^{-1} & 0 \\ 0 & \hat{U}\hat{T}^{-1} \end{bmatrix},
 \end{aligned}$$

and taking into account the relation

$$\begin{bmatrix} \alpha TB & \beta TB \\ \beta \hat{T}\hat{B} & \alpha \hat{T}\hat{B} \end{bmatrix} = \begin{bmatrix} T & 0 \\ 0 & \hat{T} \end{bmatrix} \begin{bmatrix} \alpha B & \beta B \\ \beta \hat{B} & \alpha \hat{B} \end{bmatrix},$$

it follows that

$$\mathbf{M}_{\text{IMEX}}^*(\alpha, \beta) = \mathbf{T} \mathbf{M}_{\text{IMEX}}(\alpha, \beta) \mathbf{T}^{-1}.$$

This relation implies that the stability properties of the transformed IMEX schemes with respect to the linear test system (23) are the same as that of the original IMEX methods. However, in general, SSP properties of transformed methods are different from SSP properties of original methods, and in Sect. 8, we will search for IMEX schemes with maximal SSP coefficients in a large class of IMEX TGLMs.

### 7 Characterization of SSP IMEX TGLMs

To investigate SSP properties of IMEX TGLMs (36), we will first reformulate these methods using the notation introduced by Spijker [44]. Define the coefficient matrices  $\mathbf{T}^* = [t_{ij}]$  and  $\mathbf{S}^* = [s_{ij}]$  by

$$\mathbf{T}^* = \begin{bmatrix} \mathbf{A}^* & \mathbf{0} \\ \mathbf{B}^* & \mathbf{0} \end{bmatrix} \in \mathbb{R}^{2(s+r) \times 2(s+r)}, \quad \mathbf{S}^* = \begin{bmatrix} \mathbf{U}^* \\ \mathbf{V}^* \end{bmatrix} \in \mathbb{R}^{2(s+r) \times 2r}.$$

Then (11) can be written in the form

$$\begin{cases} Y_i^{[n+1]} = h \sum_{j=1}^{2(s+r)} t_{ij} F(Y_j^{[n+1]}) + \sum_{j=1}^{2r} s_{ij} \bar{y}_j^{[n]}, & i = 1, 2, \dots, 2(s+r), \\ \bar{y}_i^{[n+1]} = h \sum_{j=1}^{2(s+r)} t_{2s+i,j} F(Y_j^{[n+1]}) + \sum_{j=1}^{2r} s_{2s+i,j} \bar{y}_j^{[n]}, & i = 1, 2, \dots, 2r, \end{cases} \tag{37}$$

$n = 0, 1, \dots, N - 1$ . Observe that

$$\bar{y}_i^{[n+1]} = Y_{2s+i}^{[n+1]}, \quad i = 1, 2, \dots, 2r.$$

In what follows, we will always assume that  $p = q$  and  $r = s$ . It follows from the preconsistency conditions that

$$\mathbf{U}^* \mathbf{q}_0^* = \begin{bmatrix} U^* & 0 \\ 0 & \hat{U}^* \end{bmatrix} \begin{bmatrix} q_0^* & 0 \\ 0 & \hat{q}_0^* \end{bmatrix} = \begin{bmatrix} U^* q_0^* & 0 \\ 0 & \hat{U}^* \hat{q}_0^* \end{bmatrix} = \begin{bmatrix} UT^{-1}Tq_0 & 0 \\ 0 & \hat{U}\hat{T}^{-1}\hat{T}\hat{q}_0 \end{bmatrix} = \begin{bmatrix} e & 0 \\ 0 & e \end{bmatrix}$$

and the coefficient matrix  $\mathbf{S}^*$  satisfies

$$\sum_{j=1}^{2r} s_{ij} = 1, \quad i = 1, 2, \dots, 2s$$

as required in [44].

We describe next the characterization of SSP coefficient  $\mathcal{C} = \mathcal{C}(\mathbf{S}^*, \mathbf{T}^*)$  of GLMs (37) which was discovered by Spijker in his seminal paper [44]. Denote by  $\mathbf{I}$  the identity matrix of dimension  $2(s+r) \times 2(s+r)$  and by

$$[\mathbf{S}^* | \gamma \mathbf{T}^*] \in \mathbb{R}^{2(s+r) \times (2r+(2s+2r))}$$

the matrix whose first  $2r$  columns are equal to  $\mathbf{S}^*$  and the last  $2(s+r)$  columns are equal to  $\gamma \mathbf{T}^*$ . Following [44] consider the condition

$$\det(\mathbf{I} + \gamma \mathbf{T}^*) \neq 0 \quad \text{and} \quad (\mathbf{I} + \gamma \mathbf{T}^*)^{-1} [\mathbf{S}^* | \gamma \mathbf{T}^*] \geq 0, \tag{38}$$

where the inequality in (38) should be interpreted componentwise. Then it was demonstrated by Spijker [44] that the SSP coefficient of GLM (37) is given by

$$\mathcal{C} = \mathcal{C}(\mathbf{S}^*, \mathbf{T}^*) = \sup \left\{ \gamma \in \mathbb{R} : \gamma \text{ satisfies (38)} \right\}. \tag{39}$$

This condition can be reformulated in terms of coefficient matrices  $\mathbf{A}^*$ ,  $\mathbf{U}^*$ ,  $\mathbf{B}^*$ , and  $\mathbf{V}^*$  of TGLMs (37). Since

$$\mathbf{I} + \gamma \mathbf{T}^* = \left[ \begin{array}{c|c} \mathbf{I}_{2s} + \gamma \mathbf{A}^* & \mathbf{0} \\ \hline \mathbf{0} & \mathbf{I}_{2r} \end{array} \right],$$

where  $\mathbf{I}_{2s}$  and  $\mathbf{I}_{2r}$  are identity matrices of dimensions  $2s \times 2s$  and  $2r \times 2r$ , it follows from the structure of the coefficient matrix  $\mathbf{A}^*$  that the condition  $\det(\mathbf{I} + \gamma \mathbf{T}^*) \neq 0$  is automatically satisfied. It can be also verified, compare [31, 32], that the second condition of (38) is equivalent to the following inequalities of lower dimensions:

$$\begin{cases} (\mathbf{I}_{2s} + \gamma \mathbf{A}^*)^{-1} \mathbf{U}^* \geq 0, & \mathbf{I}_{2s} - (\mathbf{I}_{2s} + \gamma \mathbf{A}^*)^{-1} \geq 0, \\ \mathbf{V}^* - \gamma \mathbf{B}^* (\mathbf{I}_{2s} + \gamma \mathbf{A}^*)^{-1} \mathbf{U}^* \geq 0, & \gamma \mathbf{B}^* (\mathbf{I}_{2s} + \gamma \mathbf{A}^*)^{-1} \geq 0. \end{cases} \quad (40)$$

Hence, the SSP coefficient of GLM (11), which will be denoted now by  $\mathcal{C}_{\text{IMEX}}$ , can be expressed in terms of  $\mathbf{A}^*$ ,  $\mathbf{U}^*$ ,  $\mathbf{B}^*$ , and  $\mathbf{V}^*$  by the formula

$$\mathcal{C}_{\text{IMEX}} = \mathcal{C}_{\text{IMEX}}(\mathbf{A}^*, \mathbf{U}^*, \mathbf{B}^*, \mathbf{V}^*) = \sup \left\{ \gamma \in \mathbb{R} : \gamma \text{ satisfies (40)} \right\}. \quad (41)$$

These inequalities, reformulated in terms of coefficient matrices of explicit and diagonally implicit TGLMs (36), take the form

$$\begin{cases} (I_s + \gamma A^*)^{-1} U^* \geq 0, & I_s - (I_s + \gamma A^*)^{-1} \geq 0, \\ V^* - \gamma B^* (I_s + \gamma A^*)^{-1} U^* \geq 0, & \gamma B^* (I_s + \gamma A^*)^{-1} \geq 0, \end{cases} \quad (42)$$

and

$$\begin{cases} (I_s + \gamma \hat{A}^*)^{-1} \hat{U}^* \geq 0, & I_s - (I_s + \gamma \hat{A}^*)^{-1} \geq 0, \\ \hat{V}^* - \gamma \hat{B}^* (I_s + \gamma \hat{A}^*)^{-1} \hat{U}^* \geq 0, & \gamma \hat{B}^* (I_s + \gamma \hat{A}^*)^{-1} \geq 0, \end{cases} \quad (43)$$

where  $I_s$  is the identity matrix of dimension  $s \times s$ , and the SSP coefficients of explicit and diagonally implicit TGLMs are given by

$$\mathcal{C}_E = \mathcal{C}_E(A^*, U^*, B^*, V^*) = \sup \left\{ \gamma \in \mathbb{R} : \gamma \text{ satisfies (42)} \right\}, \quad (44)$$

and

$$\mathcal{C}_I = \mathcal{C}_I(\hat{A}^*, \hat{U}^*, \hat{B}^*, \hat{V}^*) = \sup \left\{ \gamma \in \mathbb{R} : \gamma \text{ satisfies (43)} \right\}. \quad (45)$$

It follows from the above discussion that the IMEX method (36) is SSP if and only if the explicit and diagonally implicit TGLMs are SSP, and we have

$$\mathcal{C}_{\text{IMEX}} = \min \left\{ \mathcal{C}_E, \mathcal{C}_I \right\}.$$

### 8 Construction of SSP IMEX GLMs

In this section, we describe the construction of internally consistent SSP IMEX TGLMs up to the order  $p = 4$  and stage order  $q = p$ . We assume that the vectors  $q_k$  and  $\hat{q}_k$ ,  $k = 0, 1, \dots, p$ , satisfy

$$q_0 = \hat{q}_0 = e_1, \quad q_1 = \hat{q}_1 = e_2, \quad \dots, \quad q_p = \hat{q}_p = e_{p+1},$$

where  $e_1, e_2, \dots, e_{p+1}$  are the canonical bases in  $\mathbb{R}^{p+1}$ . For such methods, the vectors  $y^{[n]}$  approximate the Nordsieck vectors  $N_{y(t_n, h)}$ ,  $n = 0, 1, \dots, N$ , defined by

$$N_{y(t, h)} = \begin{bmatrix} y(t) \\ hy'(t) \\ \vdots \\ h^p y^{(p)}(t) \end{bmatrix} \in \mathbb{R}^{2m(p+1)}.$$

It follows from the discussion in Sect. 7, in particular from the formulas (45) and (44), that implicit parts of these schemes can be obtained by solving the minimization problem

$$F_I(\gamma) := -\gamma \longrightarrow \min \tag{46}$$

with non-linear inequality constrains (43), and the implicit parts of these schemes can be obtained by solving the minimization problem

$$F_E(\gamma) := -\gamma \longrightarrow \min \tag{47}$$

with non-linear inequality constrains (42). As already mentioned in Sect. 4, we will always assume that both implicit and explicit methods have IRKS property introduced in [5, 47] (see also [36, 48]), and that implicit methods are  $A$ - and  $L$ -stable. Such methods are obtained following the algorithm for construction of formulas with IRKS presented in [5, 36, 47].

#### 8.1 SSP IMEX TGLMs with $p = q = 1$ and $r = s = 2$

If the abscissa vector is fixed a priori, the explicit and implicit methods can be constructed independently. Here, we show the results corresponding to the abscissa vector  $\mathbf{c} = [1/2, 1]^T$ .

Consider first the implicit methods with  $r = s = 2$ . Following the algorithm for construction of GLMs with IRKS, and assuming that the diagonal element  $\lambda$  of the coefficient matrix  $\hat{A}$  is equal to  $1/4$ , we obtain an  $A$ - and  $L$ -stable family of methods with  $p = q = 1$  depending on the parameter  $\hat{\beta}_1$ , appearing in the algorithm for construction of such methods. Then solving the minimization problem (46) with inequality constrains (43) with respect to  $\hat{\beta}_1$  and coefficients of the transformation matrix  $\hat{T}$  defined in Sect. 6 we obtain the method with coefficients

$$\hat{A}^* = \begin{bmatrix} \frac{1}{4} & 0 \\ \frac{1}{2} & \frac{1}{4} \end{bmatrix}, \quad \hat{U}^* = \begin{bmatrix} \frac{1}{2} & \frac{1}{2} \\ \frac{1}{2} & \frac{1}{2} \end{bmatrix}, \quad \hat{B}^* = \begin{bmatrix} \frac{11}{16} & \frac{3}{16} \\ \frac{9}{16} & \frac{9}{16} \end{bmatrix}, \quad \hat{V}^* = \begin{bmatrix} \frac{1}{2} & \frac{1}{2} \\ \frac{1}{2} & \frac{1}{2} \end{bmatrix}.$$

The transformation matrix  $\hat{T}$  is

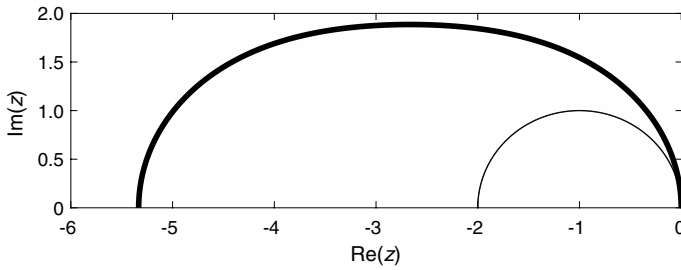


**Fig. 1** Stability region  $S_E$  (thick line) of explicit GLM with  $p = q = 1, s = r = 2$ , and stability region of RK method of order  $p = 1$  (Euler method, thin line)

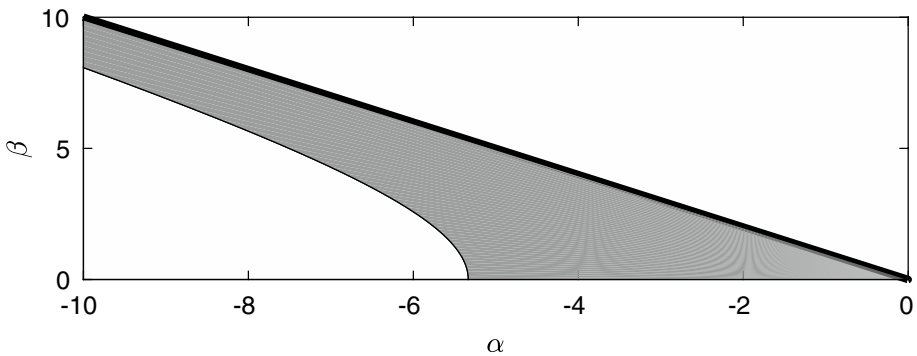


**Fig. 2** Stability region  $A_{IMEX}$  (shaded region) of IMEX method with  $p = q = 1$  and  $s = r = 2$ . The boundary  $\beta = -\alpha, \alpha \leq 0$ , of stability region of the test system (23) is plotted by a thick line

$$\hat{T} = \begin{bmatrix} 1 & \frac{1}{8} \\ 1 & \frac{1}{8} \end{bmatrix}.$$

For this method,  $C_I = 2$  and  $C_{I,eff} = 1$ .

Consider next the explicit methods with  $r = s = 2$ . Following again the algorithm for construction of GLMs with IRKS presented in [5, 36, 47], we obtain a family of methods with  $p = q = 1$  depending on the parameter  $\beta_1$  appearing in the algorithm for construction of such methods. Then, assuming that the method is internally consistent with the implicit formula, and solving the minimization problem (47) with inequality constrains (42), with respect to  $\beta_1$ , and coefficients of the transformation matrix  $T$  defined in Sect. 6, we obtain the method with coefficients

$$\hat{A}^* = \begin{bmatrix} 0 & 0 \\ \frac{1}{2} & 0 \end{bmatrix}, \quad \hat{U}^* = \begin{bmatrix} 0 & 1 \\ 0 & 1 \end{bmatrix}, \quad \hat{B}^* = \begin{bmatrix} \frac{1}{2} & \frac{1}{2} \\ \frac{1}{2} & \frac{1}{2} \end{bmatrix}, \quad \hat{V}^* = \begin{bmatrix} 0 & 1 \\ 0 & 1 \end{bmatrix}.$$

The transformation matrix  $T$  is

$$\hat{T} = \begin{bmatrix} 1 & \frac{1}{4} \\ 1 & \frac{1}{2} \end{bmatrix}.$$



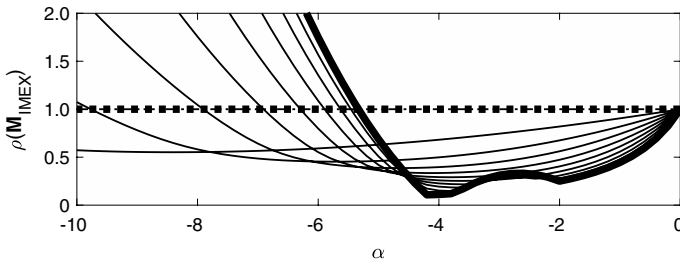


**Fig. 3** Spectral radius  $\rho(\mathbf{M}_{\text{IMEX}})$  of the stability matrix  $\mathbf{M}_{\text{IMEX}}(\alpha, \beta)$  versus  $\alpha$  for  $\beta = s\alpha$ ,  $s = 0, -0.1, -0.2, \dots, -1$ , for IMEX method with  $p = q = 1, r = s = 2$

For this method,  $C_E = 2, C_{E,\text{eff}} = 1$ , and the region of absolute stability is plotted in Fig. 1.

It follows from the discussion presented in Sect. 7 that the SSP coefficients for the resulting IMEX scheme are  $C_{\text{IMEX}} = 2$  and  $C_{\text{IMEX,eff}} = 1$ . Stability region  $\mathcal{A}_{\text{IMEX}}$  defined in Sect. 4 of the resulting IMEX scheme is plotted in Fig. 2. We have also plotted on this figure by a thick line the boundary  $\beta = -\alpha, \alpha \leq 0$ , of stability region of the test system (23). This region is symmetric with respect to  $\alpha$  axis. We have also plotted on Fig. 3 spectral radius  $\rho(\mathbf{M}_{\text{IMEX}})$  of the stability matrix  $\mathbf{M}_{\text{IMEX}}(\alpha, \beta)$  versus  $\alpha$  for  $\alpha \in [-10, 0]$  and  $\beta = s\alpha$ , for  $s = 0, -0.1, -0.2, \dots, -1$ . The spectral radius  $\rho(\mathbf{M}_{\text{IMEX}})$  is plotted by thick solid line for  $s = 0$ , thick dotted line for  $s = -1$ , and by thin solid lines for the remaining values of  $s$ . The line corresponding to  $\rho(\mathbf{M}_{\text{IMEX}}) = 1$  is plotted by a thin dash-dot line. For comparison we have also plotted on Fig. 4 stability region  $\mathcal{A}_E$  of the numerical scheme, where both equations of (23) are treated by the explicit GLM. As before, we have also plotted by a thick line the boundary  $\beta = -\alpha, \alpha \leq 0$ , of stability region of the test system (23). We can see that this region is bounded, and the region  $\mathcal{A}_{\text{IMEX}}$  is unbounded for  $\alpha \leq 0$ , and  $\alpha \approx \beta$  or  $\alpha \approx -\beta$ . Observe that stability intervals on Figs. 1, 2, 3, 4 are the same. This is a consequence of the fact that for  $b = 0$  or  $\beta = 0$  the test system (23) reduces to (22) with  $\text{Re}(\lambda) = a$  or  $\text{Re}(z) = a$ .

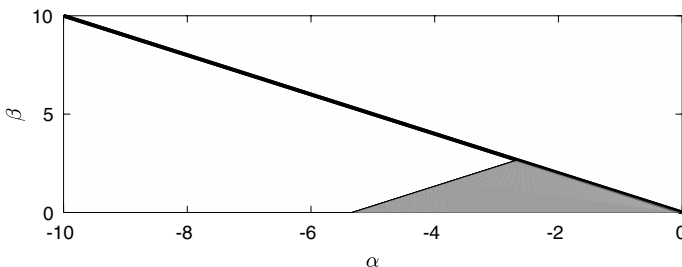


**Fig. 4** Stability region  $\mathcal{A}_E$  (shaded region) of numerical scheme, where both equations of (23) are treated by explicit GLM with  $p = q = 1$  and  $r = s = 2$ . The boundary  $\beta = -\alpha, \alpha \leq 0$ , of stability region of the test system (23) is plotted by a thick line

### 8.2 SSP IMEX GLMs with $p = q = 2$ and $r = s = 3$

If the abscissa vector is fixed a priori, the explicit and implicit methods can be constructed independently. Here, we show the results corresponding to the linearly spaced abscissa vector  $\mathbf{c} = [0, 1/2, 1]^T$ .

Consider first the implicit methods with  $r = s = 3$ . Following the algorithm for construction of GLMs with IRKS presented in [5, 36, 47], and assuming that  $\eta = 0$ , we obtain a possibly  $A$ - and  $L$ -stable family of methods with  $p = q = 2$  depending on  $\lambda, \hat{\beta}_1, \hat{\beta}_2$ , and  $\hat{l}_{21}$ . Then, solving the minimization problem (46) with inequality constrains (43) and coefficients of the transformation matrix  $\hat{T}$  defined in Sect. 6, we obtain the method with coefficients

$$\begin{aligned} \hat{A}^* &= \begin{bmatrix} 0.250000000000000000 & 0 & 0 \\ 0.5003387283822169862 & 0.250000000000000000 & 0 \\ 0.5001608898707649718 & 0.4986805982048520783 & 0.250000000000000000 \end{bmatrix}, \\ \hat{U}^* &= \begin{bmatrix} 0.3705342371692555270 & 0.1050889479918137073 & 0.3072597415271085156 \\ 0.3682704654193326803 & 0.1028456108965995988 & 0.3111307157553221749 \\ 0.3709718504031393211 & 0.1180363277649080382 & 0.2966918642404505521 \end{bmatrix}, \\ \hat{B}^* &= \begin{bmatrix} 0.7551430607053234987 & 0.4608768636120115309 & 0.0736774793781561972 \\ 0.4567582133180009406 & 0.5521438901947252606 & 0.1108288368927108960 \\ 0.7635183122245887399 & 0.4750615478256855031 & 0.0770554015207384577 \end{bmatrix}, \\ \hat{V}^* &= \begin{bmatrix} 0.4716719406013863856 & 0.1350416611974712775 & 0.3866163381775349129 \\ 0.3969003577040184400 & 0.1137194881040167662 & 0.3254203681855260268 \\ 0.5060891815952526207 & 0.1446933576732365024 & 0.4146085712945968481 \end{bmatrix}. \end{aligned}$$

The transformation matrix  $\hat{T}$  is

$$\hat{T} = \begin{bmatrix} 1.2681702121727689017 & -0.2952489424125132929 & -0.0347194343068768467 \\ 1.0673505106783030249 & -0.2142326109921935994 & 0.0674663104035160707 \\ 1.3601937352707475494 & -0.3843220008144882292 & 0.0187944424217467570 \end{bmatrix}.$$

For this method  $C_l = 2.131$  and  $C_{l,eff} = 0.710$ .

Consider next the explicit methods with  $r = s = 3$ . Following again the algorithm for construction of GLMs with IRKS presented in [5, 36, 47], assuming that the diagonal element  $\lambda$  of the coefficient matrix  $\hat{A}$  is equal to  $1/4$  and that  $\eta = 1/6$ , we obtain a family of methods with  $p = q = 2$  depending on the parameters  $\beta_1$  and  $\beta_2, l_{21}$ , appearing in the algorithm for construction of such methods. Then, solving the minimization problem (47) with inequality constrains (42), with respect to  $\beta_1, \beta_2, l_{21}$ , and coefficients of the transformation matrix  $T$  defined in Sect. 6 we obtain the method with coefficients

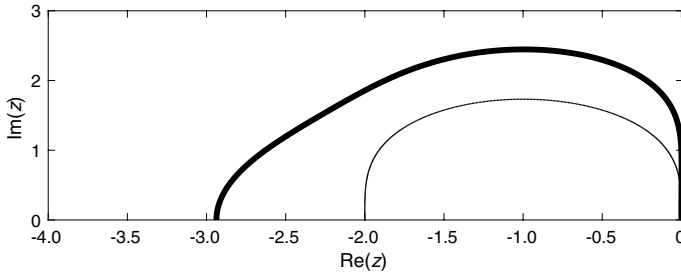


**Fig. 5** Stability region  $\mathcal{S}_E$  (thick line) of explicit GLM with  $p = q = 2, s = r = 3$ , and stability region of RK method of order  $p = 2$  (thin line)

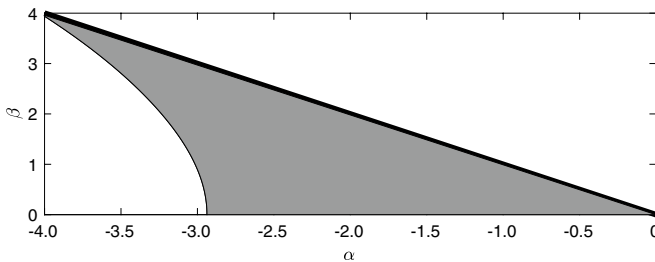


**Fig. 6** Stability region  $\mathcal{A}_{\text{IMEX}}$  (shaded region) of IMEX method with  $p = q = 2$  and  $s = r = 3$ . The boundary  $\beta = -\alpha, \alpha \leq 0$ , of stability region of the test system (23) is plotted by a thick line

$$\begin{aligned}
 A^* &= \begin{bmatrix} 0 & 0 & 0 \\ 0.6704674902497747642 & 0 & 0 \\ 0.5494708312040104825 & 0.6847019200200990196 & 0 \end{bmatrix}, \\
 U^* &= \begin{bmatrix} 0.0209453989827169455 & 1.0232147047274957245 & 0.0000211517264798749 \\ 0.0928178311311476482 & 0.8184384243551088424 & 0.0000169186248225953 \\ 0.0810400964297409653 & 0.6777134409604051812 & 0.0472758400760015948 \end{bmatrix}, \\
 B^* &= \begin{bmatrix} 0.8473330378069255943 & 0.4178144660625222059 & 7.1820389839911238\text{E}-16 \\ 0.5241364260829281828 & 0.2561049940932673033 & 0.2836402593863833120 \\ 0.8705962631349037964 & 1.0881220253044566810 & 0.1120600348024297485 \end{bmatrix}, \\
 V^* &= \begin{bmatrix} 0.0590876538224310731 & 1.0343378708912136997 & 0.4465136326910933477 \\ 0.0396957007456304837 & 0.7987551432756890163 & 0.0238991552259111082 \\ 0.1386804803714356719 & 2.7684496655871123027 & 0.1421572029018799106 \end{bmatrix}.
 \end{aligned}$$

The transformation matrix  $T$  is

$$T = \begin{bmatrix} 2.6310696125102805274 & -2.2410989322808015008 & 1.6433477499119608817 \\ 0.9233831030164229762 & 0.0459123052284078019 & -0.0336603153961643013 \\ 3.4053064855122751573 & -1.7698102004690786300 & 1.0001731955353854162 \end{bmatrix}.$$

For this method  $C_E = 1.193, C_{E,\text{eff}} = 0.398$ , and the region of absolute stability is plotted in Fig 5.

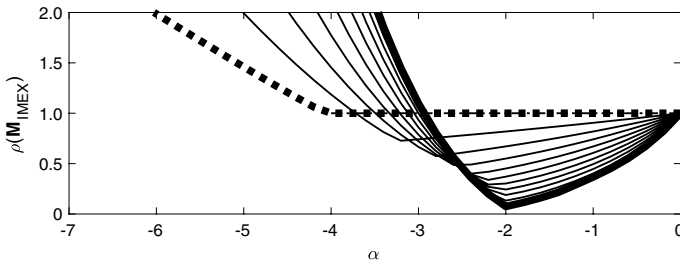


**Fig. 7** Spectral radius  $\rho(\mathbf{M}_{\text{IMEX}})$  of the stability matrix  $\mathbf{M}_{\text{IMEX}}(\alpha, \beta)$  versus  $\alpha$  for  $\beta = s\alpha$ ,  $s = 0, -0.1, -0.2, \dots, -1$ , for IMEX method with  $p = q = 2, r = s = 3$

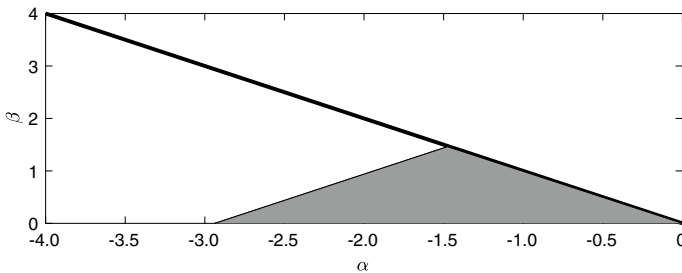


**Fig. 8** Stability region  $\mathcal{A}_E$  (shaded region) of numerical scheme, where both equations of (23) are treated by explicit GLM with  $p = q = 2$  and  $r = s = 3$ . The boundary  $\beta = -\alpha, \alpha \leq 0$ , of stability region of the test system (23) is plotted by a thick line

The SSP coefficients for the resulting IMEX scheme are  $C_{\text{IMEX}} = 1.193$  and  $C_{\text{IMEX,eff}} = 0.398$ . Stability region  $\mathcal{A}_{\text{IMEX}}$  of this IMEX scheme is plotted in Fig. 6. We have also plotted on this figure by a thick line the boundary  $\beta = -\alpha, \alpha \leq 0$ , of stability region of the test system (23). We have also plotted on Fig. 7 spectral radius  $\rho(\mathbf{M}_{\text{IMEX}})$  of the stability matrix  $\mathbf{M}_{\text{IMEX}}(\alpha, \beta)$  versus  $\alpha$  for  $\alpha \in [-4, 0]$  and  $\beta = s\alpha$ , for  $s = 0, -0.1, -0.2, \dots, -1$ . The spectral radius  $\rho(\mathbf{M}_{\text{IMEX}})$  is plotted by thick solid line for  $s = 0$ , thick dotted line for  $s = -1$ , and by thin solid lines for the remaining values of  $s$ . The line corresponding to  $\rho(\mathbf{M}_{\text{IMEX}}) = 1$  is plotted by a thin dash-dot line. For comparison we have also plotted on Fig. 8 stability region  $\mathcal{A}_E$  of the numerical scheme, where both equations of (23) are treated by the explicit GLM. As before, we have also plotted by a thick line the boundary  $\beta = -\alpha, \alpha \leq 0$ , of stability region of the test system (23).

### 8.3 SSP IMEX GLMs with $p = q = 3$ and $r = s = 4$

Here, we show the construction of methods with linearly spaced abscissa vector  $\mathbf{c} = [0, 1/3, 2/3, 1]^T$ .

Consider first the implicit methods with  $r = s = 4$ . Following the algorithm for construction of GLMs with IRKS, and assuming  $\eta = 0$ , we obtain a possibly  $A$ - and  $L$ -stable family of methods with  $p = q = 3$  depending on  $\lambda$ , and additional parameters  $\hat{\beta}_1, \hat{\beta}_2, \hat{\beta}_3$ , and  $\hat{l}_{21}, \hat{l}_{31}, \hat{l}_{32}$ . Then solving the minimization problem (46) with inequality constrains (43), additional

inequality constrain  $\gamma \leq 3/2$ , with respect to  $\lambda, \hat{\beta}_1, \hat{\beta}_2, \hat{\beta}_3, \hat{l}_{21}, \hat{l}_{31}, \hat{l}_{32}$ , and coefficients of the transformation matrix  $\hat{T}$  defined in Sect. 6 we obtain the method with coefficients

$$\hat{A}^* = \begin{bmatrix} 0.1587582736465180787 & 0 & 0 & 0 \\ 0.3147936065099799288 & 0.1587582736465180787 & 0 & 0 \\ 0.3454858702124254731 & 0.3028923511538916698 & 0.1587582736465180787 & 0 \\ 0.3589258296379142850 & 0.2686736081830728378 & 0.3484149569958441051 & 0.1587582736465180787 \end{bmatrix}$$

$$\hat{U}^* = \begin{bmatrix} 1.2102746077476118E-8 & 0.09510798840806155 & 1.2851232821192887E-6 & 0.1717658935204507 \\ 1.8001061016348753E-6 & 0.09803358596871574 & 0.05043250838107611 & 0.1521250258248718 \\ 0.00801107232689032 & 0.07192450612527633 & 0.1440799825378817 & 0.14828278781827356 \\ 0.006251907035416157 & 0.0731325640758233 & 0.19952018754896134 & 0.13495924725222 \end{bmatrix}$$

$$\hat{B}^* = \begin{bmatrix} 3.0750880359621176089 & 1.8452080931110706230 & 3.0199868465929942814 & 3.5349711953779992129 \\ 1.4846462660473323362 & 1.2867048779875503551 & 3.5016697010508622271 & 0.0070533088914376356 \\ 0.2899078369728039130 & 0.1630440067916633232 & 0.1876341083869850912 & 0.215465693566269512 \\ 1.1439080001274604665 & 1.0468868405168857363 & 1.81734710364810256E-7 & 2.9887342577642890E-7 \end{bmatrix}$$

$$\hat{V}^* = \begin{bmatrix} 0.0646577804346853480 & 0.5701051519984964510 & 1.5995011697914174392 & 1.1030790328948990606 \\ 0.0432799312149678904 & 0.3613254821543134692 & 0.9595956756554017304 & 0.7071311815690112969 \\ 0.0037958447944054611 & 0.0691601073953650214 & 0.1534672318588225536 & 0.1150734456447886832 \\ 0.0279140719631941620 & 0.2101375084793350469 & 0.4860119754945125701 & 0.4205495055521786292 \end{bmatrix}$$

The transformation matrix  $\hat{T}$  is

$$\hat{T} = \begin{bmatrix} 8.1145043412098264992 & 2.2811232704776104174 & -0.0151454120576273984 & 0.0256496614792116036 \\ 5.1387798158770256149 & 0.4592389089894047285 & -0.1614483011681006885 & -0.0933880056895376061 \\ 0.8608233077554180325 & -0.1180960808570202895 & 0.0964536057858727941 & -0.0269331048442746026 \\ 2.9764918627879737515 & -1.1785543344490776459 & 0.0893943440680522027 & 0.0517097980423208014 \end{bmatrix}$$

For this method  $C_I = 1.51$  and  $C_{I,eff} = 0.38$ .

Consider next the explicit methods with  $r = s = 4$ . Following again the algorithm for construction of GLMs with IRKS, and assuming  $\eta = 1/24$ , we obtain a family of methods with  $p = q = 3$  depending on the parameters  $\beta_1$  and  $\beta_2, \beta_3, l_{21}, l_{31}$ , and  $l_{32}$  appearing in the algorithm for construction of such methods. Then, assuming that the method is internally consistent with the implicit formula, and solving the minimization problem (47) with inequality constrains (42), with respect to  $\beta_1, \beta_2, \beta_3, l_{21}, l_{31}, l_{32}$ , and coefficients of the transformation matrix  $T$  defined in Sect. 6, we obtain the method with coefficients

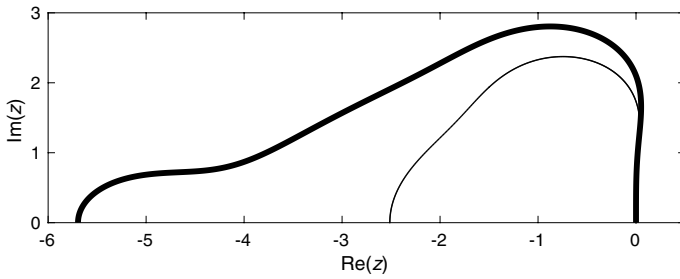


**Fig. 9** Stability region  $\mathcal{S}_E$  (thick line) of explicit GLM with  $p = q = 3, s = r = 4$ , and stability region of RK method of order  $p = 3$  (thin line)

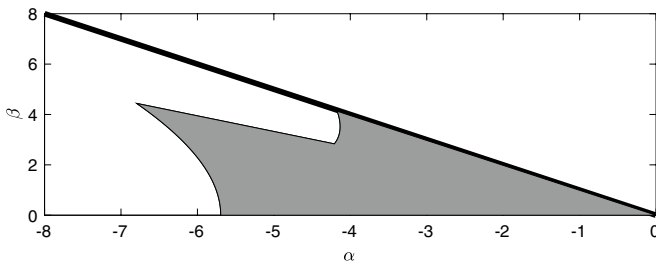


**Fig. 10** Stability region  $\mathcal{A}_{\text{IMEX}}$  (shaded region) of IMEX method with  $p = q = 3$  and  $s = r = 4$ . The boundary  $\beta = -\alpha, \alpha \leq 0$ , of stability region of the test system (23) is plotted by a thick line

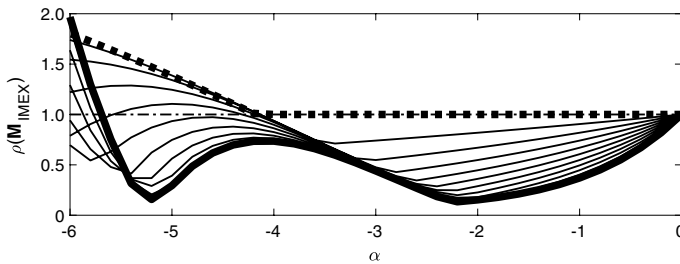


**Fig. 11** Spectral radius  $\rho(\mathbf{M}_{\text{IMEX}})$  of the stability matrix  $\mathbf{M}_{\text{IMEX}}(\alpha, \beta)$  versus  $\alpha$  for  $\beta = s\alpha, s = 0, -0.1, -0.2, \dots, -1$ , for IMEX method with  $p = q = 3, r = s = 4$

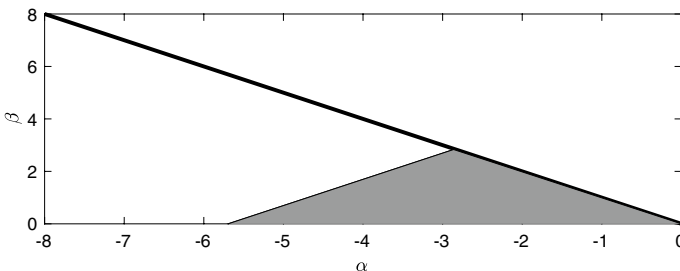


**Fig. 12** Stability region  $\mathcal{A}_E$  (shaded region) of numerical scheme, where both equations of (23) are treated by explicit GLM with  $p = q = 3$  and  $r = s = 4$ . The boundary  $\beta = -\alpha, \alpha \leq 0$ , of stability region of the test system (23) is plotted by a thick line

$$\begin{aligned}
 A^* &= \begin{bmatrix} 0 & 0 & 0 & 0 \\ 0.5015095193979003096 & 0 & 0 & 0 \\ 0.3509907446284340617 & 0.5131855222025055076 & 0 & 0 \\ 0.2639478681292023099 & 0.3886688787223385316 & 0.5125407700599630123 & 0 \end{bmatrix}, \\
 U^* &= \begin{bmatrix} 0.0009458256048679615 & 0.1214065990432195876 & 0.1130202511459750579 & 0.0050812239544181834 \\ 0.0005888717568407858 & 0.0902775318063270008 & 0.0703665492976113533 & 0.0395610633040175212 \\ 0.0102745857744406272 & 0.0796000995468820021 & 0.0492473538418985049 & 0.0430982309858525754 \\ 0.0180937297751885805 & 0.0818334750346923066 & 0.0454737598765323415 & 0.0347921276431494769 \end{bmatrix}, \\
 B^* &= \begin{bmatrix} 2.2523296901935043401 & 3.4841041337806903118 & 2.1095408916438571722 & 0.2828744206433550248 \\ 2.0266130529703889071 & 1.1693636869010657149 & 1.7365291750506974032 & 0.8169626379955447777 \\ 1.3710912691067697903 & 0.9340310971745189184 & 1.0075419617259765482 & 0.4119239972830878316 \\ 2.3043455790790701248 & 2.1974986473423812329 & 0.5687494664546820081 & 0.0039757675493384804 \end{bmatrix}, \\
 V^* &= \begin{bmatrix} 0.0839854310784300597 & 1.3332465780780297849 & 0.4161471500438139899 & 0.2218548862816888858 \\ 0.0460850398016848498 & 0.3884292884391450126 & 0.2929123438994835803 & 0.1081374169435784128 \\ 0.0198429714688718073 & 0.2576947981446385273 & 0.4012379283837833029 & 0.1233403363848953670 \\ 0.4699603258691165015 & 0.3997486346842408621 & 0.3233631438416656100 & 0.1263473520986416248 \end{bmatrix}.
 \end{aligned}$$

The transformation matrix  $T$  is

$$T = \begin{bmatrix} 9.9312154657332446400 & -2.0146699867246063439 & -0.3988369450540766616 & 0.9947940272446191511 \\ 4.1571133295008636574 & 1.1048113490974887666 & -0.7167913653652819087 & 0.4047371530992648852 \\ 3.9085442387259372084 & -0.9421513049687170538 & 0.6916877872459864308 & -0.443375486600909206 \\ 8.6910476438960921177 & -5.0664338248695413190 & 1.8156461397803871157 & 0.0062476888389285992 \end{bmatrix}.$$

For this method  $C_E = 1.24$ ,  $C_{E,\text{eff}} = 0.31$ , and the region of absolute stability is plotted in Fig 9.

The SSP coefficients for the resulting IMEX scheme are  $C_{\text{IMEX}} = 1.24$  and  $C_{\text{IMEX,eff}} = 0.31$ . Stability region  $\mathcal{A}_{\text{IMEX}}$  of the resulting IMEX scheme is plotted in Fig. 10. This region is bounded and extends to about  $\alpha = \pm\beta = -4.15$  along the lines  $\beta = \pm\alpha$ . We have also plotted on this figure by a thick line the boundary  $\beta = -\alpha$ ,  $\alpha \leq 0$ , of stability region of the test system (23). We have also plotted on Fig. 11 spectral radius  $\rho(\mathbf{M}_{\text{IMEX}})$  of the stability matrix  $\mathbf{M}_{\text{IMEX}}(\alpha, \beta)$  versus  $\alpha$  for  $\alpha \in [-6, 0]$  and  $\beta = s\alpha$ , for  $s = 0, -0.1, -0.2, \dots, -1$ . The spectral radius  $\rho(\mathbf{M}_{\text{IMEX}})$  is plotted by thick solid line for  $s = 0$ , thick dotted line for  $s = -1$ , and by thin solid lines for the remaining values of  $s$ . The line corresponding to  $\rho(\mathbf{M}_{\text{IMEX}}) = 1$  is plotted by a thin dash-dot line. For comparison we have also plotted on Fig. 12 stability region  $\mathcal{A}_E$  of the numerical scheme, where both equations of (23) are treated by the explicit GLM. As before, we have also plotted by a thick line the boundary  $\beta = -\alpha$ ,  $\alpha \leq 0$ , of stability region of the test system (23).

### 8.4 SSP IMEX GLMs with $p = q = 4$ and $r = s = 5$

Here, we show the construction of methods with linearly spaced abscissa vector  $\mathbf{c} = [0, 1/4, 1/2, 3/4, 1]^T$ .

Consider first the implicit methods with  $r = s = 5$ . Following the algorithm for construction of GLMs with IRKS, and assuming that  $\eta = 0$ , we obtain a possibly  $A$ - and  $L$ -stable family of methods with  $p = q = 4$  depending on  $\hat{\beta}_1, \hat{\beta}_2, \hat{\beta}_3, \hat{\beta}_4$ , and  $\hat{l}_{21}, \hat{l}_{31}, \hat{l}_{32}, \hat{l}_{41}, \hat{l}_{42}, \hat{l}_{43}$ . Then, solving the minimization problem (46) with inequality constrains (43), additional inequality

constrains  $\gamma \leq 3/2$ , with respect to  $\lambda, \hat{\beta}_1, \hat{\beta}_2, \hat{\beta}_3, \hat{\beta}_4, \hat{l}_{21}, \hat{l}_{31}, \hat{l}_{32}, \hat{l}_{41}, \hat{l}_{42}, \hat{l}_{43}$ , and coefficients of the transformation matrix  $\hat{T}$  defined in Sect. 6 we obtain the method with coefficients

$$\hat{A}^* = \begin{bmatrix} 0.1026541498671639909 & 0 & 0 & 0 & 0 \\ 0.2104155077712366174 & 0.1026541498671639909 & 0 & 0 & 0 \\ 0.1804998115106030666 & 0.2534396011077829942 & 0.1026541498671639909 & 0 & 0 \\ 0.2003687340719781937 & 0.2439474023536451122 & 0.2682968838612916433 & 0.1026541498671639909 & 0 \\ 0.2149197220271112059 & 0.1581215733769807394 & 0.3172668506621374553 & 0.2501678379902111984 & 0.1026541498671639909 \end{bmatrix},$$

$$\hat{U}^* = \begin{bmatrix} 0.0017507900134227017 & 6.7318737597927559E-6 & 0.0082536311487357817 & 0.0025916661167807678 & 0.0889139326544405459 \\ 0.0019218950799270200 & 0.0153852640332281136 & 0.0033976988086306140 & 0.0007088417863984310 & 0.0798426778368396765 \\ 0.0017364066200722539 & 0.0292329576498193698 & 0.0118118331818167014 & 0.0006080626386883765 & 0.0580697654240866400 \\ 0.0017802957004428544 & 0.0197052651766038336 & 0.0123868943992437104 & 0.0045691459046282445 & 0.0630724894349725606 \\ 0.0019580780478763794 & 0.0295676070591021954 & 0.0190222957547033207 & 0.0019903154389705835 & 0.0491617451510652119 \end{bmatrix},$$

$$\hat{B}^* = \begin{bmatrix} 1.1468433169622039047 & 2.3405008080551537294 & 1.7841703189743897771 & 0.4311585694294190066 & 1.3259069005534106168 \\ 2.0078700993191591248 & 2.7420623489697215595 & 1.7184046037628132188 & 1.3041945818295646563 & 4.0106835821401073206 \\ 1.4965888464053731523 & 3.6965462647148686951 & 2.5218698514795293370 & 0.2407683861233892659 & 0.7404154461834526408 \\ 2.2482095497141571747 & 2.6022072354803587441 & 1.0770223349882140535 & 0.4094948656674662311 & 1.2592862733592327402 \\ 2.2202097581748032127 & 1.5616721955831628766 & 3.2880560875611528866 & 2.364913544779883497 & 0.0707859309044374350 \end{bmatrix},$$

$$\hat{V}^* = \begin{bmatrix} 0.0841806297003035179 & 0.1445868040035408743 & 0.0597211973759077311 & 0.0883875633999846101 & 0.6227081135575271315 \\ 0.0164710882084377213 & 0.2717470552864313290 & 0.1775186015447681358 & 0.0462095028803371321 & 0.4988856025358828410 \\ 0.0249505576198493679 & 0.2488324478642199359 & 0.1028214020821387652 & 0.0829039865553031797 & 0.5066858592053278452 \\ 0.0125590807458929075 & 0.3048632723463564468 & 0.0618426050649928313 & 0.0361814272630941736 & 0.5918787314136294937 \\ 0.0134457748882583137 & 0.2815712602369490900 & 0.1247424628839976307 & 0.0770881278411806196 & 0.5050694856680322144 \end{bmatrix}.$$

The transformation matrix  $\hat{T}$  is

$$\hat{T} = \begin{bmatrix} 9.8676314416359738694 & -3.8337896663560231320 & 2.2828585446599413632 & -0.9963640019082533808 & 0.3990323296250162779 \\ 9.9438557561834643654 & 1.3287941157362032311 & 0.3494284712595161364 & 0.0088497314991052999 & -0.0193471432429202003 \\ 9.5299909846460711572 & -1.4079148066903179087 & -0.0945342619447120952 & 0.0741972063564250021 & 0.0108235351662332993 \\ 9.9508781269033486420 & -2.6971995980785123385 & 0.5964460283973141386 & 0.0578375764252724983 & -0.059853799389977968 \\ 9.877085607444001632 & -0.8698331280516334402 & -0.0535877352562708953 & 0.0110452038173330995 & -0.0071159149018987998 \end{bmatrix}.$$

For this method  $C_I = 1.50$  and  $C_{I,eff} = 0.30$ .

Consider next the explicit methods with  $r = s = 5$ . Following again the algorithm for construction of GLMs with IRKS, assuming  $\eta = 1/120$ , we obtain a family of methods with  $p = q = 4$  depending on the parameters  $\beta_1$  and  $\beta_2, \beta_3, \beta_4, l_{21}, l_{31}, l_{32}, l_{41}, l_{42}, l_{43}$ , appearing in the algorithm for construction of such methods. Then, assuming that the method is internally consistent with the implicit formula, and solving the minimization problem (47) with inequality constrains (42), with respect to  $\beta_1, \beta_2, \beta_3, \beta_4, l_{21}, l_{31}, l_{32}, l_{41}, l_{42}, l_{43}$ , and coefficients of the transformation matrix  $T$  defined in Sect. 6 we obtain the method with coefficients



$$\begin{aligned}
 A^* &= \begin{bmatrix} 0 & 0 & 0 & 0 & 0 \\ 0.4417111030737873338 & 0 & 0 & 0 & 0 \\ 0.1644343031042212071 & 0.4670483511022344381 & 0 & 0 & 0 \\ 0.1187370743815824674 & 0.3141283116784794731 & 0.4264255194988550945 & 0 & 0 \\ 0.3040093516679691182 & 0.1045601034886504757 & 0.1442055205755064217 & 0.5216743019921853023 & 0 \end{bmatrix} \\
 U^* &= \begin{bmatrix} 0.0076806958523112218 & 0.0478701592959415731 & 0.0241709637804630051 & 0.0010308738787743445 & 0.0381561234137053128 \\ 0.0022634097775238769 & 0.0686580863412751056 & 0.0130415986469209753 & 0.0247862415621660135 & 0.0106358678427780174 \\ 0.0087427810827810142 & 0.0652183806083473705 & 0.0139297728377206279 & 0.0228954050304003819 & 0.0072834932535713101 \\ 0.0209069931254498558 & 0.0676293150628618826 & 0.0056344241585976988 & 0.0136600748981572729 & 0.0110825948120292142 \\ 0.0100241092868467783 & 0.0575852115944299527 & 0.0160960448723609398 & 0.0052610767269572500 & 0.0309069335078178293 \end{bmatrix} \\
 B^* &= \begin{bmatrix} 4.8819612887953393642 & 5.0043090699215476939 & 2.0995165692335877709 & 6.8617502191233721408 & 0.0011234657325213515 \\ 1.9206733619511261488 & 0.4821259078151781854 & 1.6331758837459723527 & 0.0003381339665351838 & 1.3002243537592648E-8 \\ 1.5030209051013873098 & 2.2971252767163813125 & 5.0172927322943649209 & 3.5055420003915285753 & 3.9177525501767901933 \\ 1.5486640271260079534 & 3.1570183970553966590 & 4.5974747524186174491 & 0.8162059845956186543 & 0.0000130076581489195 \\ 1.3377503680409932720 & 4.5363835052551853105 & 0.8692321023640166183 & 3.2156629072829075608 & 0.0408453755572449678 \end{bmatrix} \\
 V^* &= \begin{bmatrix} 0.1132616353927589386 & 0.6248876336617833866 & 0.1114608438338539979 & 0.1208357248037200834 & 0.2224463199955226397 \\ 0.0560706772836316892 & 0.5817947723551945359 & 0.0434324775608005962 & 0.0857375633501667642 & 0.1540455505806404501 \\ 0.0782693037783967266 & 0.6967440452100281788 & 0.0875617105558678103 & 0.1635292391804090357 & 0.1267132706668479554 \\ 0.3699451490453822815 & 0.3083386489780842917 & 0.2717050114372367676 & 0.0973196856754897895 & 0.0507366091716716645 \\ 0.1382837896426468020 & 0.3819407511844215204 & 0.1672277493321670036 & 0.1613457684349285468 & 0.1200621960206889257 \end{bmatrix}
 \end{aligned}$$

The transformation matrix  $T$  is

$$T = \begin{bmatrix} 9.9732827471037548802 & 7.7604409358255184833 & -5.2750271211949624960 & 2.1565953647775586647 & -0.7017935910636133101 \\ 7.4995710528317202341 & -5.3616956666003137596 & 3.1165918247111466515 & -1.6684153192062349780 & 0.8309449754965087017 \\ 9.5508859592357649431 & 4.7345376332878284716 & 0.5797129982138089796 & -1.0253011334005798258 & 0.6474740453290085368 \\ 9.9999974288807748108 & 3.023455590554425134 & -5.8839911389117435802 & 4.1263562371023380415 & -2.0325937343364021657 \\ 8.4712414148115809235 & 2.0836629359772343458 & -3.0564540330561087510 & 2.1970763858800745705 & -1.2564675035475039096 \end{bmatrix}$$

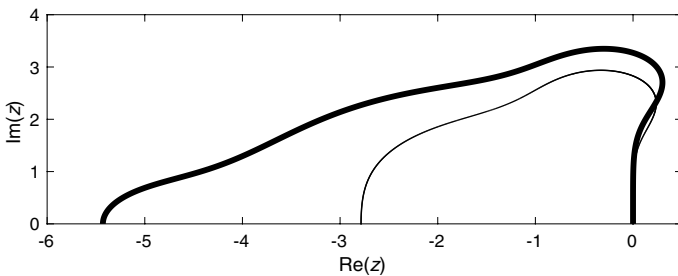


**Fig. 13** Stability region  $S_E$  (thick line) of explicit GLM with  $p = q = 4$ ,  $s = r = 5$ , and stability region of RK method of order  $p = 4$  (thin line)

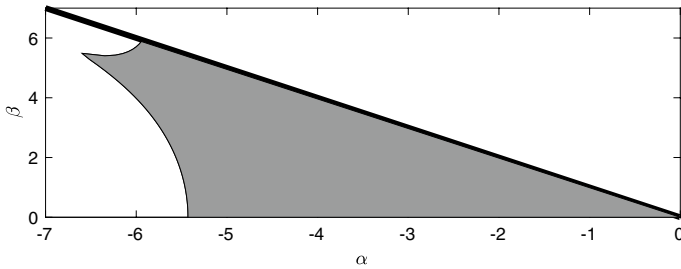


**Fig. 14** Stability region  $\mathcal{A}_{\text{IMEX}}$  (shaded region) of IMEX method with  $p = q = 4$  and  $s = r = 5$ . The boundary  $\beta = -\alpha, \alpha \leq 0$ , of stability region of the test system (23) is plotted by a thick line

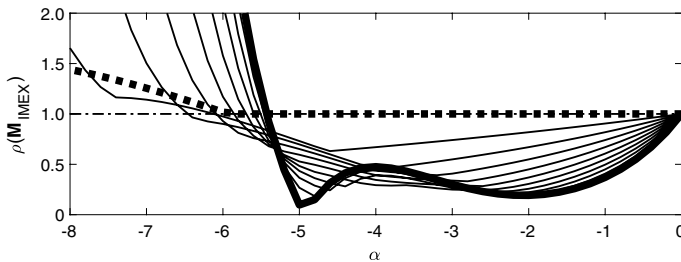


**Fig. 15** Spectral radius  $\rho(\mathbf{M}_{\text{IMEX}})$  of the stability matrix  $\mathbf{M}_{\text{IMEX}}(\alpha, \beta)$  versus  $\alpha$  for  $\beta = s\alpha, s = 0, -0.1, -0.2, \dots, -1$ , for IMEX method with  $p = q = 4, r = s = 5$

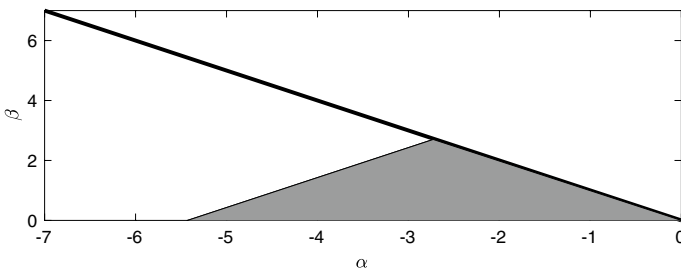


**Fig. 16** Stability region  $\mathcal{A}_E$  (shaded region) of numerical scheme, where both equations of (23) are treated by explicit GLM with  $p = q = 4$  and  $r = s = 5$ . The boundary  $\beta = -\alpha, \alpha \leq 0$ , of stability region of the test system (23) is plotted by a thick line

For this method  $C_E = 0.63, C_{E,\text{eff}} = 0.13$ , and the region of absolute stability is plotted in Fig 13.

The SSP coefficients for the resulting IMEX scheme are  $C_{\text{IMEX}} = 0.63$  and  $C_{\text{IMEX,eff}} = 0.13$ . Stability region  $\mathcal{A}_{\text{IMEX}}$  of the resulting IMEX scheme is plotted in Fig. 14. This region is bounded and extends to about  $\alpha = \pm\beta = -6.00$  along the lines  $\beta = \pm\alpha$ . We have also plotted on this figure by a thick line the boundary  $\beta = -\alpha, \alpha \leq 0$ , of stability region of the test system (23). We have also plotted on Fig. 15 spectral radius  $\rho(\mathbf{M}_{\text{IMEX}})$  of the stability matrix  $\mathbf{M}_{\text{IMEX}}(\alpha, \beta)$  versus  $\alpha$  for  $\alpha \in [-8, 0]$  and  $\beta = s\alpha$ , for  $s = 0, -0.1, -0.2, \dots, -1$ . The spectral radius  $\rho(\mathbf{M}_{\text{IMEX}})$  is plotted by thick solid line for

$s = 0$ , thick dotted line for  $s = -1$ , and by thin solid lines for the remaining values of  $s$ . The line corresponding to  $\rho(\mathbf{M}_{\text{IMEX}}) = 1$  is plotted by a thin dash-dot line. For comparison we have also plotted on Fig. 16 stability region  $\mathcal{A}_E$  of the numerical scheme, where both equations of (23) are treated by the explicit GLM. As before, we have also plotted by a thick line the boundary  $\beta = -\alpha$ ,  $\alpha \leq 0$ , of stability region of the test system (23).

### 9 Starting and Finishing Procedures

To start the integration with IMEX method (36), we have to compute the starting vectors

$$\bar{x}^{[0]} = (T \otimes I)x^{[0]}, \quad \bar{z}^{[0]} = (\hat{T} \otimes I)z^{[0]},$$

where

$$x^{[0]} = \sum_{k=0}^p (q_k \otimes I)h^k x^{(k)}(t_0) + O(h^{p+1}), \quad z^{[0]} = \sum_{k=0}^p (\hat{q}_k \otimes I)h^k z^{(k)}(t_0) + O(h^{p+1}).$$

This can be done in many different ways and in what follows, we describe the strategy to compute  $x^{[0]}$  and  $z^{[0]}$  using initial values  $x_0 = x(t_0)$  and  $z_0 = z(t_0)$  and approximations  $x_k$  and  $z_k$  of order  $p$  to  $x(t_0 + kh)$  and  $z(t_0 + kh)$ ,  $k = 1, 2, \dots, p$ . This strategy was first suggested in the context of diagonally implicit multistage integration methods by Butcher [3], and then described in more detail in [6, 7] in the context of GLMs.

Putting

$$Q = [q_0 \ q_1 \ \dots \ q_p] \in \mathbb{R}^{r \times (p+1)}, \quad \hat{Q} = [\hat{q}_0 \ \hat{q}_1 \ \dots \ \hat{q}_p] \in \mathbb{R}^{r \times (p+1)},$$

we have

$$x^{[0]} = (Q \otimes I)N_x(t_0, h) + O(h^{p+1}), \tag{48}$$

$$z^{[0]} = (\hat{Q} \otimes I)N_z(t_0, h) + O(h^{p+1}), \tag{49}$$

where  $N_x(t, h)$  and  $N_z(t, h)$  are Nordsieck vectors corresponding to  $x(t)$  and  $z(t)$ , i.e.,

$$N_x(t, h) = \begin{bmatrix} x(t) \\ hx'(t) \\ \vdots \\ h^p x^{(p)}(t) \end{bmatrix}, \quad N_z(t, h) = \begin{bmatrix} z(t) \\ hz'(t) \\ \vdots \\ h^p z^{(p)}(t) \end{bmatrix}.$$

For methods with  $r = p + 1$ , these Nordsieck vectors can be approximated by

$$\begin{bmatrix} x(t_0) \\ hx'(t_0) \\ \vdots \\ h^p x^{(p)}(t_0) \end{bmatrix} = (S \otimes I) \begin{bmatrix} x(t_0) \\ x(t_0 + h) \\ \vdots \\ x(t_0 + ph) \end{bmatrix} + O(h^{p+1}), \tag{50}$$

$$\begin{bmatrix} z(t_0) \\ hz'(t_0) \\ \vdots \\ h^p z^{(p)}(t_0) \end{bmatrix} = (S \otimes I) \begin{bmatrix} z(t_0) \\ z(t_0 + h) \\ \vdots \\ z(t_0 + ph) \end{bmatrix} + O(h^{p+1}), \quad (51)$$

where the matrix  $S$  can be obtained by expanding  $x(t_0 + kh)$  and  $z(t_0 + kh)$  into Taylor series around  $t_0$  and comparing terms of the same order on both sides of the resulting relations. The matrices  $S$  corresponding to  $p = 1, 2, 3$ , and  $4$ , are listed in [6, 7] but to make this paper self-contained these matrices are also listed below. We have

$$S = \begin{bmatrix} 1 & 0 \\ -1 & 1 \end{bmatrix}, \quad S = \begin{bmatrix} 1 & 0 & 0 \\ -\frac{3}{2} & 2 & -\frac{1}{2} \\ 1 & -2 & 1 \end{bmatrix}$$

for  $p = 1$  and  $p = 2$ , and

$$S = \begin{bmatrix} 1 & 0 & 0 & 0 \\ -\frac{11}{6} & 3 & -\frac{3}{2} & \frac{1}{3} \\ 2 & -5 & 4 & -1 \\ -1 & 3 & -3 & 1 \end{bmatrix}, \quad S = \begin{bmatrix} 1 & 0 & 0 & 0 & 0 \\ -\frac{25}{12} & 4 & -3 & \frac{4}{3} & -\frac{1}{4} \\ \frac{35}{12} & -\frac{26}{3} & \frac{19}{2} & -\frac{14}{3} & \frac{11}{12} \\ -\frac{5}{2} & 9 & -12 & 7 & -\frac{3}{2} \\ 1 & -4 & 6 & -4 & 1 \end{bmatrix}$$

for  $p = 3$  and  $p = 4$ .

It follows from relations (48), (49), (50) and (51) that

$$x^{[0]} = (QS \otimes I) \begin{bmatrix} x(t_0) \\ x(t_0 + h) \\ \vdots \\ x(t_0 + ph) \end{bmatrix} + O(h^{p+1}),$$

$$z^{[0]} = (\widehat{Q}S \otimes I) \begin{bmatrix} z(t_0) \\ z(t_0 + h) \\ \vdots \\ z(t_0 + ph) \end{bmatrix} + O(h^{p+1}).$$

Based on these relations, we propose to compute approximations to  $x^{[0]}$  and  $z^{[0]}$  from the equations

$$x^{[0]} = (QS \otimes I) \begin{bmatrix} x_0 \\ x_1 \\ \vdots \\ x_p \end{bmatrix}, \quad z^{[0]} = (\widehat{Q}S \otimes I) \begin{bmatrix} z_0 \\ z_1 \\ \vdots \\ z_p \end{bmatrix}.$$

The approximations  $x_k$  and  $z_k$  to  $x(t_0 + kh)$  and  $z(t_0 + kh)$ ,  $k = 1, 2, \dots, p$ , can be computed by IMEX RK methods of order  $p$ , discussed, for example, in [1, 2, 8, 33, 40].

We describe now the finishing procedure following the presentation in [7]. After completing the integration with IMEX GLMs (3) and (4), we have computed the vectors

$$\bar{x}^{[N]} = (T \otimes I)x^{[N]}, \quad \bar{z}^{[N]} = (\hat{T} \otimes I)z^{[N]}.$$

We then compute

$$x^{[N]} = (T^{-1} \otimes I)\bar{x}^{[N]} = \sum_{k=0}^p (q_k \otimes I)h^k x^{(k)}(t_{\text{end}}) + O(h^p),$$

$$z^{[N]} = (\hat{T}^{-1} \otimes I)\bar{z}^{[N]} = \sum_{k=0}^p (\hat{q}_k \otimes I)h^k z^{(k)}(t_{\text{end}}) + O(h^p),$$

where  $q_k = \hat{q}_k = e_{k+1}$ ,  $k = 0, 1, \dots, p$ . These vectors approximate the Nordsieck vectors  $N_x(t_{\text{end}}, h)$  and  $N_z(t_{\text{end}}, h)$  at the endpoint  $t_{\text{end}}$  of the interval of integration, and  $x_1^{[N]}$  and  $z_1^{[N]}$  are the required approximations to  $x(t_{\text{end}})$  and  $z(t_{\text{end}})$ , i.e.,

$$x_1^{[N]} = x(t_{\text{end}}) + O(h^p), \quad z_1^{[N]} = z(t_{\text{end}}) + O(h^p).$$

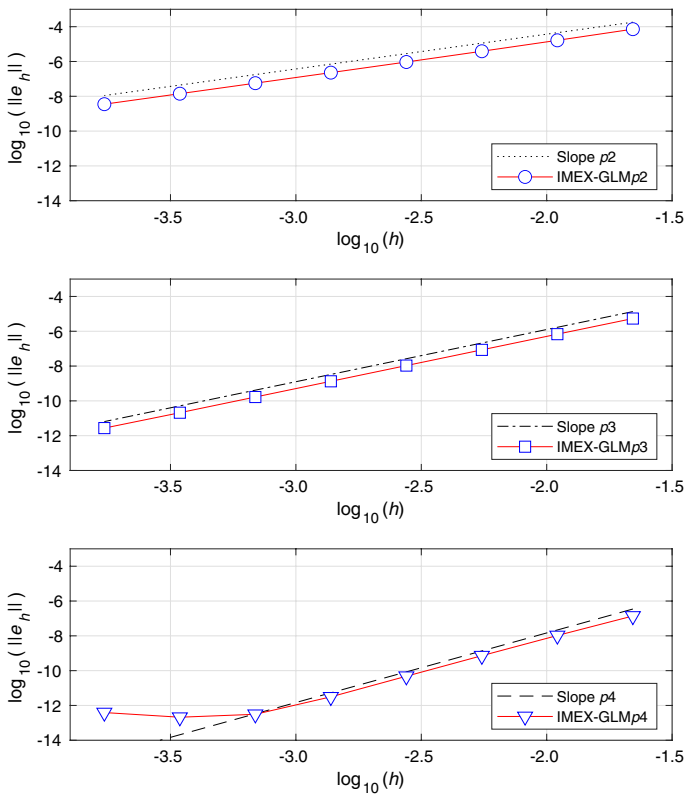


**Fig. 17** Error versus stepsize (double logarithmic scale plot) for IMEX-GLMp2, IMEX-GLMp3 and IMEX-GLMp4 applied to problem (52)

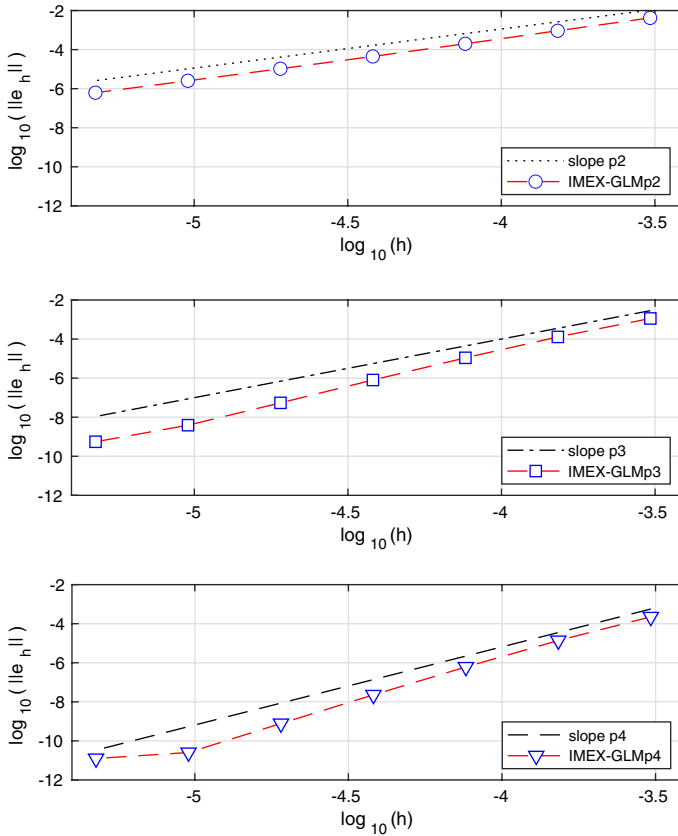


**Fig. 18** Error versus stepsize (double logarithmic scale plot) for IMEX-GLMp2, IMEX-GLMp3 and IMEX-GLMp4 applied to problem (53)

## 10 Numerical Experiments

### 10.1 ODEs

We now test the methods derived in Sect. 8 on four examples of ordinary partitioned systems of differential equations. The results reported in this section have been obtained using the starting procedure described in Sect. 9. All the approximations to the solution at linearly spaced points, needed for the starting procedure, and all the reference solutions, have been computed by Matlab code `ode15s` with  $\text{AbsTol} = \text{eps}$  and  $\text{RelTol} = 10^2 * \text{eps}$ , where  $\text{eps}$  stands for double precision machine Epsilon, i.e.,  $\text{eps} \approx 2.22 * 10^{-16}$ . For each selected test, we have plotted in double logarithmic scale the maximum of the infinity norm of the global error all over the integration grid, versus the stepsize  $h$  (see Figs. 17, 18, 19, 20).

**Example 1** ([22]) The van der Pol equation:

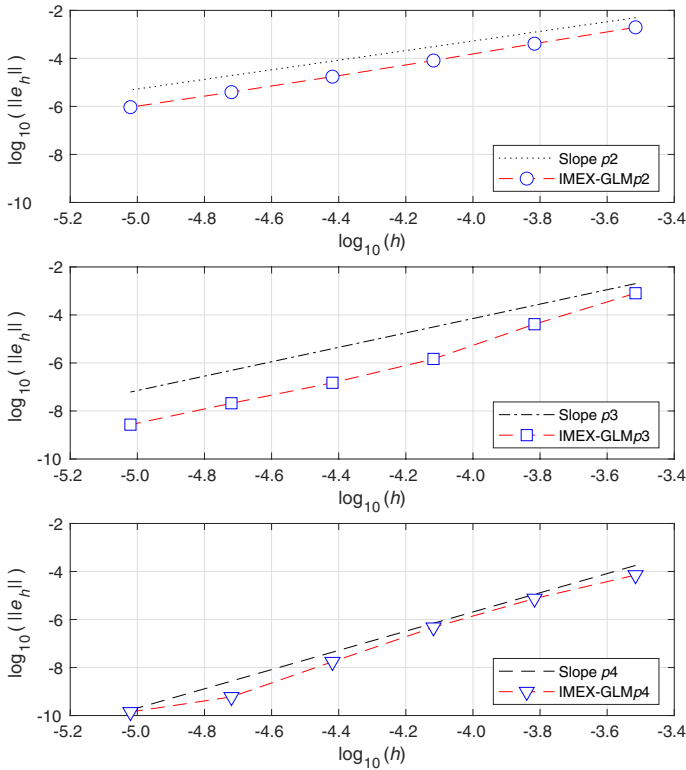


**Fig. 19** Error versus stepsize (double logarithmic scale plot) for IMEX-GLMp2, IMEX-GLMp3 and IMEX-GLMp4 applied to problem (54)

$$\begin{cases} x'(t) = z(t), \\ z'(t) = \left( (1 - x(t)^2)z(t) - x(t) \right) / \epsilon, \end{cases} \tag{52}$$

$t \in [0, t_{\text{end}}], t_{\text{end}} = 0.55139, 0 < \epsilon \ll 1$ , with initial conditions

$$x(0) = 2, \quad z(0) = -\frac{2}{3} + \frac{10}{81} \epsilon - \frac{292}{2187} \epsilon^2 - \frac{1814}{19683} \epsilon^3 + O(\epsilon^4).$$

We consider here a stiff case where  $\epsilon = 10^{-6}$ .

**Example 2** ([27, 46]) Problem in biochemistry:

$$\begin{cases} x'(t) = (z(t) - 1)x(t) + 0.99z(t), \\ z'(t) = 1000(x(t) - z(t) - x(t)z(t)), \end{cases} \tag{53}$$

$t \in [0, t_{\text{end}}], t_{\text{end}} = 50$ . The initial conditions are

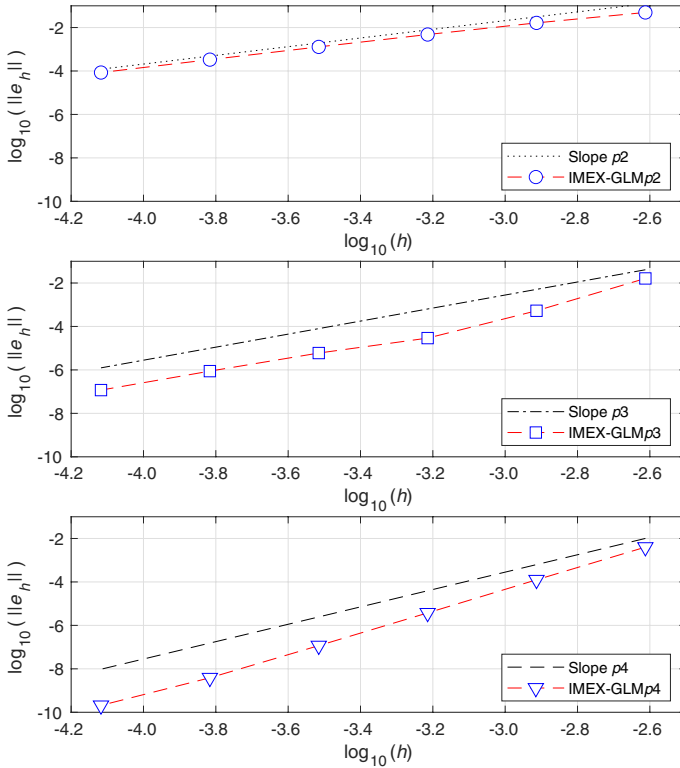


**Fig. 20** Error versus stepsize (double logarithmic scale plot) for IMEX-GLMp2, IMEX-GLMp3 and IMEX-GLMp4 applied to problem (55)

$$x(0) = 1, \quad z(0) = 0.$$

**Example 3** ([11, 27]) Nonlinear chemical problem of Robertson:

$$\begin{cases} x_1'(t) = -0.04x_1(t) + 0.01x_2(t)z(t), \\ x_2'(t) = 30z(t)^2, \\ z'(t) = 400x_1(t) - 100x_2(t)z(t) - 3\,000z(t)^2, \end{cases} \quad (54)$$

$t \in [0, t_{\text{end}}]$ ,  $t_{\text{end}} = 5$ . The initial conditions are

$$x_1(0) = 1, \quad x_2(0) = 0, \quad z(0) = 0.$$

**Example 4** The differential system from [27]:



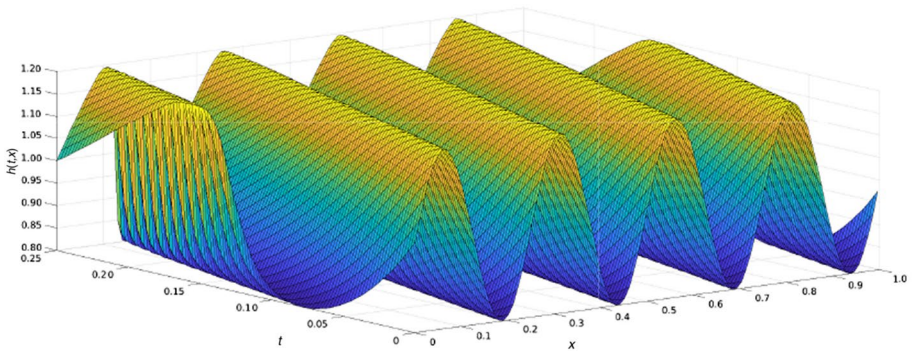


**Fig. 21** Evolution of the shallow water model (56), with  $\varepsilon = 10^{-8}$  and  $t \in [0, 0.25]$

$$\begin{cases} x_1'(t) = 0.1(z_1(t) - x_1(t)), \\ x_2'(t) = 0.87(z_2(t) - x_2(t)) - 11(x_2(t) - x_3(t)), \\ x_3'(t) = 1.8(x_2(t) - x_3(t)) - 13(x_3(t) - 270), \\ z_1'(t) = 250((R(t) - 1)z_1(t) + x_1(t)), \\ z_2'(t) = 93z_1(t) - 0.26(z_2(t) - x_2(t)), \end{cases} \tag{55}$$

$t \in [0, t_{\text{end}}]$ ,  $t_{\text{end}} = 10$ . The function  $R(t)$  is defined by

$$R(t) = -0.0048(z_2(t) - 660.2) - 0.032(x_3(t) - 273.9),$$

and the initial conditions are

$$x_1(0) = 1, \quad x_2(0) = 302.2, \quad x_3(0) = 223.9, \quad z_1(0) = 1, \quad z_2(0) = 660.2.$$

We applied the methods of order  $p = 2$ ,  $p = 3$ , and  $p = 4$  introduced in Sect. 8 to problems (52)–(55). Figures 17, 18, 19, 20 confirm that all methods achieve the expected order of convergence for large range of stepsizes. We note a limiting accuracy of  $10^{-12}$  for the method order  $p = 4$  when applied to the van der Pol problem (52).

### 10.2 Semi-discretized Partial Differential Equations

We now test the methods derived in Sect. 8 on two examples of ordinary partitioned systems of differential equations arising from spatial discretization of partial differential equations.

**Example 5** Shallow water model [38, 40].

We consider a one-dimensional model of shallow water flow:

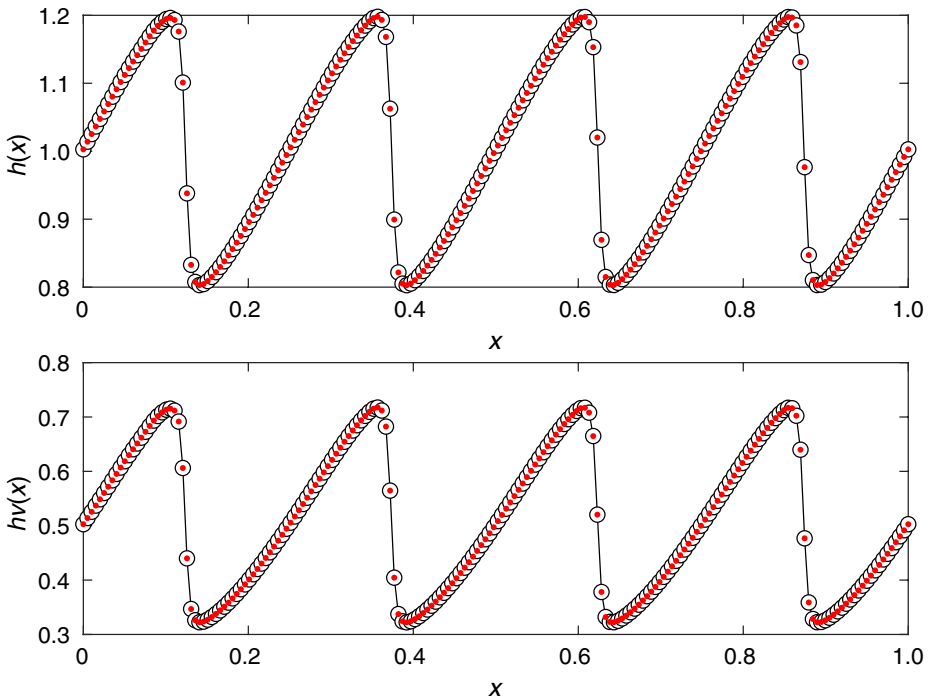


**Fig. 22** Numerical solution to shallow water model, (56) with  $\epsilon = 10^{-8}$  and  $t \in [0, 0.25]$ , computed by IMEX-GLMp3, for  $N = 200$  spatial points, and  $h = 1/200$ . Reference solution (black circles) and numerical solution computed by IMEX-GLMp3 (red dots)

$$\begin{cases} \frac{\partial}{\partial t} h + \frac{\partial}{\partial x} (hv) = 0, \\ \frac{\partial}{\partial t} (hv) + \frac{\partial}{\partial x} \left( h + \frac{1}{2} h^2 \right) = \frac{1}{\epsilon} \left( \frac{h^2}{2} - hv \right), \end{cases} \tag{56}$$

where  $h$  is the water height with respect to the bottom and  $hv$  is the flux of the velocity field. We use periodic boundary conditions and initial conditions at  $t_0 = 0$

$$h(0, x) = 1 + \frac{1}{5} \sin(8\pi x), \quad hv(0, x) = \frac{1}{2} h(0, x)^2 \tag{57}$$

with  $x \in [0, 1]$ . For this problem the space derivative has been discretized by a fifth order finite difference weighted essentially non-oscillatory (WENO) scheme following the implementation described in [42]. The evolution of the model is shown in Figs. 21 and 22.

To verify the experimental order of the proposed methods, we considered the case with  $N = 100$  spatial points, that results in a system of first-order ODEs of dimension  $d = 200$ . The first hundred components, corresponding to  $h_r$ , are integrated by the explicit method, while the rest of the components, corresponding to  $(hv)_r$ , are integrated by the implicit method.

The numerical results with  $\epsilon = 10^{-2}$  and  $\epsilon = 10^{-8}$ , reported in Figs. 23 and 24, confirm that the methods proposed in this paper have the asymptotic preserving property, but they are also asymptotically accurate in the stiff limit for  $\epsilon \rightarrow 0$  (compare [40]). In other words, for

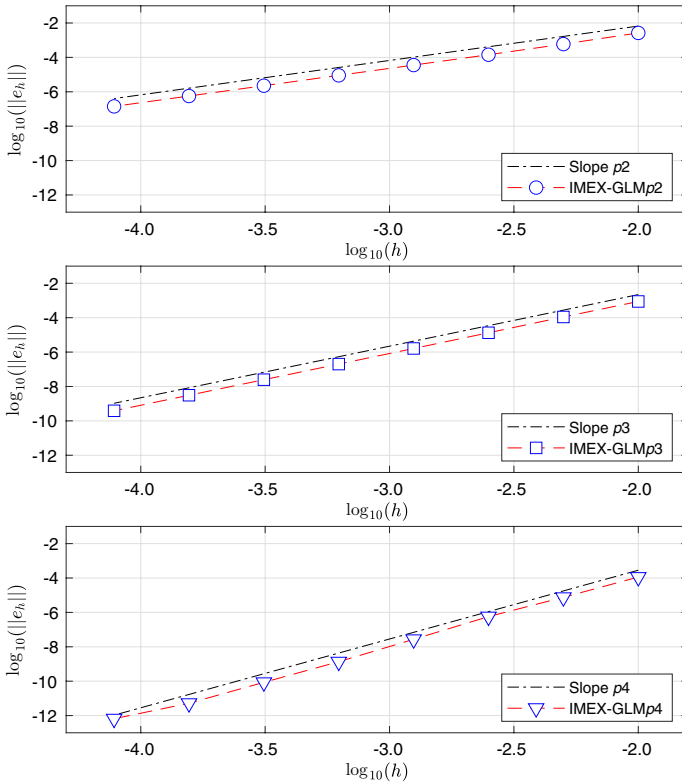


**Fig. 23** Error versus stepsize (double logarithmic scale plot) for IMEX-GLMp2, IMEX-GLMp3 and IMEX-GLMp4 applied to the discretization of the shallow water problem (56), with  $N = 100$ , by a WENO5 space discretization scheme, and  $\epsilon = 10^{-2}$

small values of  $\epsilon$  the expected order of convergence matches the theoretical one and no order reduction occurs (compare [33, 35]).

**Example 6** Population dynamics model — positivity test ([26, 29]).

We consider the evolution of a population density  $P$  according to the model

$$\frac{\partial P(t, x)}{\partial t} = f(t, x) + b(x, P(t, x)) - r_d P(t, x) + d \frac{\partial^2 P(t, x)}{\partial x^2}, \tag{58}$$

where  $x \in [0, 1]$  and  $t \geq 0$ . We assume periodic boundary conditions and zero initial condition,  $P(0, x) = 0, x \in [0, 1]$ .

This differential equation models the evolution of an ecological population using birth, death and migration. A description of the model can be found in [29]. The birth rate,  $b(x, P)$ , has taken to decline nonlinearly with the population density:

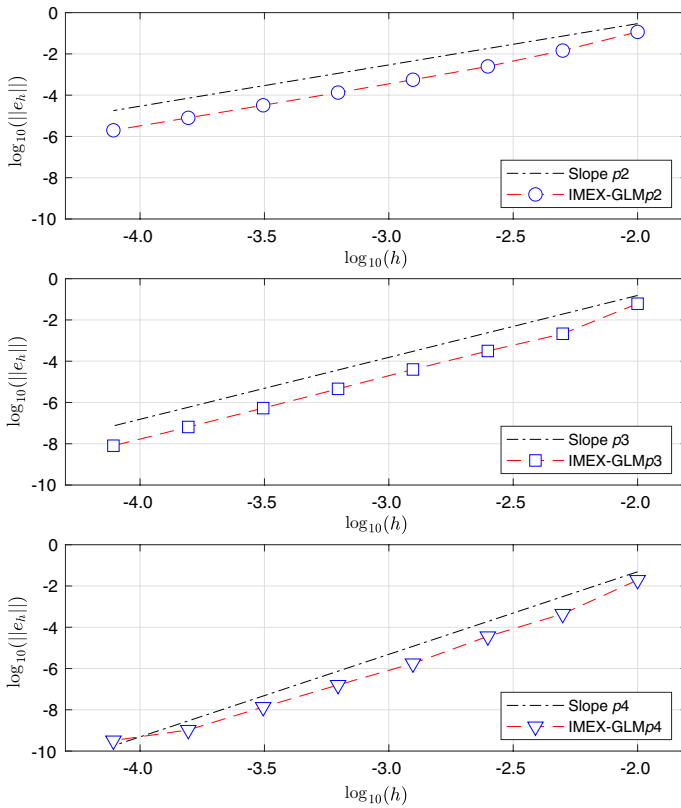


**Fig. 24** Error versus stepsize (double logarithmic scale plot) for IMEX-GLMp2, IMEX-GLMp3 and IMEX-GLMp4 applied to the discretization of the shallow water problem (56), with  $N = 100$ , by a WENO5 space discretization scheme, and  $\epsilon = 10^{-8}$

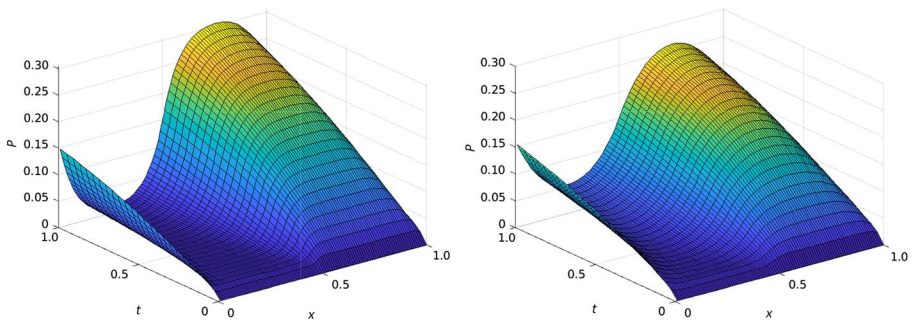


**Fig. 25** Evolution of the population dynamics model (58), with  $d = 0.01$  (left) and  $d = 0.04$  (right), for  $t \in [0, 1]$ . Numerical solution computed by IMEX-GLMp3

**Fig. 26** Steady state (computed at  $t = 10$ ) of the population dynamics model (58), with  $d = 0.01$  and  $d = 0.04$

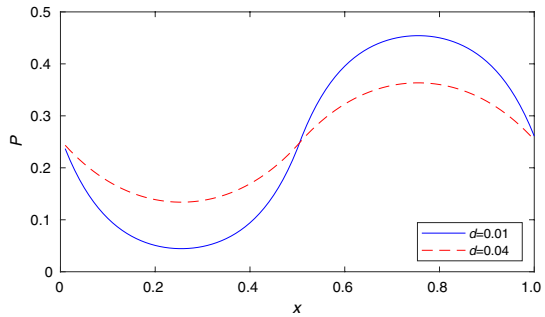


**Table 1** Problem (58) — critical time step values for positivity preservation

Method	$\bar{h}(d = 0)$	$\bar{h}(d = 0.01)$	$\bar{h}(d = 0.04)$
IMEX-GLMp2	1.202 3	1.185 5	1.264 4
IMEX-GLMp3	1.345 6	1.352 8	2.567 3
IMEX-GLMp4	1.160 2	1.354 6	2.626 3

$$b(x, P) = r_b(x) \frac{\epsilon}{\epsilon + P}, \quad \epsilon = 0.005.$$

The death rate is set equal to one, i.e.,  $r_d = 1$ . The birth rate  $r_b$  varies by position according to

$$r_b(x) = \begin{cases} 1 & \text{if } x \in [0, 1/2], \\ 100 & \text{if } x \in (1/2, 1]. \end{cases}$$

The forcing term,  $f(t, x)$ , is taken to be zero for all times  $t \neq 0$ . At time  $t = 0$ , and for each grid point,  $f$  is assigned a random value in the interval  $[0.8, 1.2]$  according to a uniform distribution. Finally, note that we treat models with diffusion,  $d = 0.01, 0.04$ , and without,  $d = 0$ . Without diffusion, the population eventually must tend to zero in the first half of the domain. Conversely, the diffusive model evolves as shown in Fig. 25 and tends to a non-zero profile as  $t$  increases, see Fig. 26.

In all cases, the analytical solution is non-negative for all times  $t \neq 0$ .

For these tests, we set  $Dx = 1/100$  and use second-order centered differences to discretize the diffusion term. The problem is reformulated as (1), where stiff diffusion term is treated implicitly, while the other terms are treated explicitly.

As stated in [29], the preservation of positivity is particularly desirable in this problem since it leads to more biologically meaningful population densities and avoids the possibility of having reaction terms grow unboundedly (which would happen for  $P$  tending to  $-\epsilon$ ). Examples of IMEX methods which, for some choice of the stepsize  $h$ , return negative approximations that cause huge error can be found in [29].

We have experimentally determined the largest step size  $\bar{h}$  for which the numerical solution maintains the positivity (at least) up to  $t = 10$ . The results reported in Table 1 show that the proposed IMEX-GLMs methods preserve the positivity of the numerical solution for larger stepsizes with respect to methods analyzed in [29].

## 11 Concluding Remarks

We considered the integration of partitioned systems of ODEs, with stiff and nonstiff components, by IMEX general linear methods. For this class of methods we provide formulation, order and stage order conditions, as well as a characterization of SSP IMEX GLMs. We then analyzed the stability of these methods with respect to two, uncoupled and coupled, linear test systems, and we introduced a suitable transformation which does not modify the order, the stage order and the linear stability properties of the methods, but allow to obtain methods with larger SSP coefficients. Afterwards, we showed how to determine good methods inside the considered class, and provided examples of methods of order  $p = 1, 2, 3$  and  $p = 4$ . Finally, after giving information about the starting and the finishing procedure, we reported the results of numerical tests on a selection of stiff problems, that confirm the good performance of the methods here introduced.

**Funding** Open access funding provided by Università degli Studi di Napoli Federico II within the CRUI-CARE Agreement.

**Open Access** This article is licensed under a Creative Commons Attribution 4.0 International License, which permits use, sharing, adaptation, distribution and reproduction in any medium or format, as long as you give appropriate credit to the original author(s) and the source, provide a link to the Creative Commons licence, and indicate if changes were made. The images or other third party material in this article are included in the article's Creative Commons licence, unless indicated otherwise in a credit line to the material. If material is not included in the article's Creative Commons licence and your intended use is not permitted by statutory regulation or exceeds the permitted use, you will need to obtain permission directly from the copyright holder. To view a copy of this licence, visit <http://creativecommons.org/licenses/by/4.0/>.

## References

1. Asher, U.M., Ruuth, S.J., Spiteri, R.J.: Implicit-explicit Runge-Kutta methods for time-dependent partial differential equations. *Appl. Numer. Math.* **25**, 151–167 (1997)
2. Asher, U.M., Ruuth, S.J., Wetton, B.: Implicit-explicit methods for time dependent PDE's. *SIAM J. Numer. Anal.* **32**, 797–823 (1995)
3. Butcher, J.C.: Diagonally-implicit multi-stage integration methods. *Appl. Numer. Math.* **11**, 347–363 (1993)
4. Butcher, J.C., Jackiewicz, Z.: Diagonally implicit general linear methods for ordinary differential equations. *BIT* **33**, 452–472 (1993)
5. Butcher, J.C., Wright, W.M.: The construction of practical general linear methods. *BIT* **43**, 695–721 (2003)
6. Califano, G., Izzo, G., Jackiewicz, Z.: Starting procedures for general linear methods. *Appl. Numer. Math.* **120**, 165–175 (2017)
7. Califano, G., Izzo, G., Jackiewicz, Z.: Strong stability preserving general linear methods with Runge-Kutta stability. *J. Sci. Comput.* **76**, 943–968 (2018)
8. Cardone, A., Jackiewicz, Z., Sandu, A., Zhang, H.: Extrapolated implicit-explicit Runge-Kutta methods. *Math. Model. Anal.* **19**, 18–43 (2014)
9. Conde, S., Gottlieb, S., Grant, Z.J., Shadid, J.N.: Implicit and implicit-explicit strong stability preserving Runge-Kutta methods with high linear order. *J. Sci. Comput.* **73**, 667–690 (2017)
10. Constantinescu, E.M., Sandu, A.: Optimal strong-stability-preserving general linear methods. *SIAM J. Sci. Comput.* **32**, 3130–3150 (2010)
11. Enright, W.H.: Second derivative multistep methods for stiff ordinary differential equations. *SIAM J. Numer. Anal.* **11**, 321–331 (1974)
12. Ferracina, L., Spijker, M.N.: An extension and analysis of the Shu-Osher representation of Runge-Kutta methods. *Math. Comput.* **74**, 201–219 (2004)

13. Ferracina, L., Spijker, M.N.: Stepsize restrictions for the total-variation-diminishing property in general Runge-Kutta methods. *SIAM J. Numer. Anal.* **42**, 1073–1093 (2004)
14. Ferracina, L., Spijker, M.N.: Stepsize restrictions for the total-variation-boundedness in general Runge-Kutta procedures. *Appl. Numer. Math.* **53**, 265–279 (2005)
15. Ferracina, L., Spijker, M.N.: Strong stability of singly-diagonally-implicit Runge-Kutta methods. *Appl. Numer. Math.* **58**, 1675–1686 (2008)
16. Gottlieb, S.: On high order strong stability preserving Runge-Kutta methods and multistep time discretizations. *J. Sci. Comput.* **25**, 105–127 (2005)
17. Gottlieb, S., Ketcheson, D.I., Shu, C.-W.: High order strong stability preserving time discretizations. *J. Sci. Comput.* **38**, 251–289 (2009)
18. Gottlieb, S., Ketcheson, D., Shu, C.-W.: *Strong Stability Preserving Runge-Kutta and Multistep Time Discretizations*. World Scientific, New Jersey (2011)
19. Gottlieb, S., Ruuth, S.J.: Optimal strong-stability-preserving time stepping schemes with fast downwind spatial discretizations. *J. Sci. Comput.* **27**, 289–303 (2006)
20. Gottlieb, S., Shu, C.-W., Tadmor, E.: Strong stability-preserving high-order time discretization methods. *SIAM Rev.* **43**, 89–112 (2001)
21. Hairer, E., Nørsett, S.P., Wanner, G.: *Solving Ordinary Differential Equations I: Nonstiff Problems*. Springer-Verlag, New York (1993)
22. Hairer, E., Wanner, G.: *Solving Ordinary Differential Equations II. Stiff and Differential-Algebraic Problems*. Springer Verlag, Berlin (1996)
23. Higueras, I.: On strong stability preserving time discretization methods. *J. Sci. Comput.* **21**, 193–223 (2004)
24. Higueras, I.: Monotonicity for Runge-Kutta methods: inner product norms. *J. Sci. Comput.* **24**, 97–117 (2005)
25. Higueras, I.: Representations of Runge-Kutta methods and strong stability preserving methods. *SIAM J. Numer. Anal.* **43**, 924–948 (2005)
26. Higueras, I., Happenhofer, N., Koch, O., Kupka, F.: Optimized strong stability preserving IMEX Runge-Kutta methods. *J. Comput. Appl. Math.* **272**, 116–140 (2014)
27. Hofer, E.: A partially implicit method for large stiff systems of ODE's with only few equations introducing small time-constants. *SIAM J. Numer. Anal.* **13**, 645–663 (1976)
28. Hundsdorfer, W., Ruuth, S.J.: On monotonicity and boundedness properties of linear multistep methods. *Math. Comput.* **75**, 655–672 (2005)
29. Hundsdorfer, W., Ruuth, S.J.: IMEX extensions of linear multistep methods with general monotonicity and boundedness properties. *J. Comput. Phys.* **225**, 2016–2042 (2007)
30. Hundsdorfer, W., Ruuth, S.J., Spiteri, R.J.: Monotonicity-preserving linear multistep methods. *SIAM J. Numer. Anal.* **41**, 605–623 (2003)
31. Izzo, G., Jackiewicz, Z.: Strong stability preserving general linear methods. *J. Sci. Comput.* **65**, 271–298 (2015)
32. Izzo, G., Jackiewicz, Z.: Strong stability preserving multistage integration methods. *Math. Model. Anal.* **20**, 552–577 (2015)
33. Izzo, G., Jackiewicz, Z.: Highly stable implicit-explicit Runge-Kutta methods. *Appl. Numer. Math.* **113**, 71–92 (2017)
34. Izzo, G., Jackiewicz, Z.: Strong stability preserving transformed DIMSIMs. *J. Comput. Appl. Math.* **343**, 174–188 (2018)
35. Izzo, G., Jackiewicz, Z.: Transformed implicit-explicit DIMSIMs with strong stability preserving explicit part. *Numer. Algorithms* **81**, 1343–1359 (2019)
36. Jackiewicz, Z.: *General Linear Methods for Ordinary Differential Equations*. John Wiley, Hoboken (2009)
37. Jackiewicz, Z., Tracogna, S.: A general class of two-step Runge-Kutta methods for ordinary differential equations. *SIAM J. Numer. Anal.* **32**, 1390–1427 (1995)
38. Jin, S.: Runge-Kutta methods for hyperbolic systems with stiff relaxation terms. *J. Comput. Phys.* **122**, 51–67 (1995)
39. Ketcheson, D.I., Gottlieb, S., Macdonald, C.B.: Strong stability preserving two-step Runge-Kutta methods. *SIAM J. Numer. Anal.* **49**, 2618–2639 (2011)
40. Pareschi, L., Russo, G.: Implicit-explicit Runge-Kutta schemes and applications to hyperbolic systems with relaxation. *J. Sci. Comput.* **25**, 129–155 (2005)
41. Ruuth, S.J., Hundsdorfer, W.: High-order linear multistep methods with general monotonicity and boundedness properties. *J. Comput. Phys.* **209**, 226–248 (2005)

42. Shu, C.-W.: High order ENO and WENO schemes for computational fluid dynamics. In: Barth, T.J., Deconinck, H. (eds) *High-Order Methods for Computational Physics*. Lecture Notes in Computational Science and Engineering, vol. 9, pp. 439–582. Springer, Berlin (1999)
43. Shu, C.-W., Osher, S.: Efficient implementation of essentially non-oscillatory shock-capturing schemes. *J. Comput. Phys.* **77**, 439–471 (1988)
44. Spijker, M.N.: Stepsize conditions for general monotonicity in numerical initial value problems. *SIAM J. Numer. Anal.* **45**, 1226–1245 (2007)
45. Spiteri, R.J., Ruuth, S.J.: A new class of optimal high-order strong-stability-preserving time discretization methods. *SIAM J. Numer. Anal.* **40**, 469–491 (2002)
46. Van der Houwen, P.J.: Explicit Runge-Kutta formulas with increased stability boundaries. *Numer. Math.* **20**, 149–164 (1972)
47. Wright, W.: *General linear methods with inherent Runge-Kutta stability*. Ph.D. thesis. The University of Auckland, New Zealand (2002)
48. Wright, W.: Explicit general linear methods with inherent Runge-Kutta stability. *Numer. Algorithms* **31**, 381–399 (2002)
49. Zhang, H., Sandu, A., Blaise, S.: Partitioned and implicit-explicit general linear methods for ordinary differential equations. *J. Sci. Comput.* **61**, 119–144 (2014)